SANDIA REPORT SAND81-1873 • Unlimited Release • UC-70
Printed March 1982

Thermal Conductivity, Bulk Properties, and Thermal Stratigraphy of Silicic Tuffs From the Upper Portion of Hole USW-G1, Yucca Mountain, Nye County, Nevada

Allen R. Lappin, R. G. VanBuskirk, D. O. Enniss, S. W. Butters,
F. M. Prater, C. B. Muller, and J. L. Bergosh

Prepared by
Sandia National Laboratories
Albuquerque, New Mexico 87185 and Livermore, California 94550
for the United States Department of Energy
under Contract DE-AC04-76DP00789

SF2900Q(8-81)

DISCLAIMER

Issued by Sandia National Laboratories, operated for the United States Department of Energy by Sandia Corporation.

Printed in the United States of America
Available from
National Technical Information Service
U.S. Department of Commerce
5285 Port Royal Road
Springfield, VA 22161

NTIS price codes
Printed copy: A03
Microfiche copy: A01

PAGES 1 to 2

WERE INTENTIONALLY

LEFT BLANK

SAND81-1873
Unlimited Release
Printed March 1982

SAND--81-1873

DE82 013387

Distribution
Category UC-70

Thermal Conductivity, Bulk Properties, and Thermal Stratigraphy of Silicic Tuffs From the Upper Portion of Hole USW-G1, Yucca Mountain, Nye County, Nevada

Allen R. Lappin
NNWSI Geotechnical Projects Division 4763
Sandia National Laboratories
Albuquerque, NM 87185

R. G. VanBuskirk, D. O. Enniss, S. W. Butters,
F. M. Prater, C. B. Muller, and J. L. Bergosh
Terra Tek, Inc
420 Wakara Way
Salt Lake City, UT 84108

Abstract

Thermal-conductivity and bulk-property measurements were made on welded and nonwelded silicic tuffs from the upper portion of Hole USW-G1, located near the southwestern margin of the Nevada Test Site. Bulk-property measurements were made by standard techniques. Thermal conductivities were measured at temperatures as high as 280°C, confining pressures to 10 MPa, and pore pressures to 1.5 MPa.

Extrapolation of measured saturated conductivities to zero porosity suggests that matrix conductivity of both zeolitized and devitrified tuffs is independent of stratigraphic position, depth, and probably location. This fact allows development of a thermal-conductivity stratigraphy for the upper portion of Hole G1. Estimates of saturated conductivities of zeolitized nonwelded tuffs and devitrified tuffs below the water table appear most reliable. Estimated conductivities of saturated densely welded devitrified tuffs above the water table are less reliable, due to both internal complexity and limited data presently available. Estimation of conductivity of dewatered tuffs requires use of different air thermal conductivities in devitrified and zeolitized samples. Estimated effects of in-situ fracturing generally appear negligible.

DISCLAIMER

DISCLAIMER

Portions of this document may be illegible in electronic image products. Images are produced from the best available original document.

Contents

Figures

Tables

Thermal Conductivity, Bulk Properties, and Thermal Stratigraphy of Silicic Tuffs From the Upper Portion of Hole USW-G1, Yucca Mountain, Nye County, Nevada

Introduction

The future of nuclear power depends, in part, on improved waste management. One option for terminal waste disposal would require excavation of repositories under land-base sites. Evaluation of potential repository horizons at such sites requires extensive information if the in-situ response to heating imposed by the waste is to be predicted. A mathematical model of the host rock and surrounding units is rquired for this prediction; the model requires determination of the physical, mechanical, and thermal properties of the units. At least part of the data must come from laboratory tests that duplicate the overburdens, fluid pressures, and temperatures expected to result from waste emplacement.

The program of thermal conductivity and physical property measurements described in this report was conducted at Terra Tek, Inc, Salt Lake City, Utah. The work was one of several ongoing activities aimed at determining the feasibility of siting a nuclear-waste repository in tuff either on the Nevada Test Site (NTS) or adjacent to it. This overall effort, the Nevada Nuclear Waste Storage Investigations (NNWSI) project, is administered by the Nevada Operations Office of the US Department of Energy (DOE). The general stratigraphy in the upper portion of Hole G1 is shown in Table 1, as are numbers of samples analyzed for thermal conductivity and physical properties. The static water level in G1 is at ~564 m (1850 ft) depth.

This report has three main objectives:

- To report thermal conductivities of samples of silicic tuffs from the upper portion of Hole USW-G1 (Figure 1).
- To report general physical properties of the analyzed tuffs (porosity, grain density, etc) and determine how these properties and mineralogy affect thermal conductivity.
- To develop a thermal-conductivity stratigraphy for the upper portion of Hole G1 by combining the established correlations between bulk properties, mineralogy, and thermal conductivity with additional bulk-property measurements.

Test Procedures

Sample Preparation and Bulk-Property Measurements

Standard procedures were generally used for sample preparation and bulk-property measurement, and are described in Appendix A. Care was taken to saturate samples fully by means of vacuum impregnation with water before thermal conductivity measurements.

Duplicate bulk-properties analyses were performed on 39 samples during the course of this study. The average difference between pairs of bulk-density measurements on the same sample is 0.045 g/cm^3, with ± 0.044 g/cm^3 standard deviation. This indicates that measured bulk densities should be precise to ± 0.09 g/cm^3 at the one-sigma level of confidence. Similarly, individual dry-bulk densities should be precise to ± 0.1 g/cm^3, porosities to ± 0.06, and calculated bulk densities at full saturation to ± 0.06 g/cm^3. The precision of reported grain densities depends on rock type. In zeolitic samples, in which the grain density is generally 2.5 g/cm^3 or less, measurements should be precise to ± 0.06 g/cm^3. In devitrified zeolite-free samples, measurements appear precise to ± 0.04 g/cm^3; grain densities of these samples are generally 2.6 g/cm^3 or greater. The reduced precision in zeolitized material appears to be due to the fact that zeolites will

partially rehydrate after drying if exposed to air, even for a short period of time. Given the simplicity of the individual steps involved in these measurements, the accuracy should be of the same order as the precision. Throughout this report, densities and porosities are generally reported without associated uncertainties.

Table 1. Stratigraphic Intervals and Number of Samples Tested, Upper Portion of USW-G1 (Stratigraphic intervals taken from Ref 1)

Stratigraphic Unit	Depth (m(ft))	Samples Tested to Date	
		Thermal Conductivity	Bulk Properties
Quaternary Alluvium	0-18.3 (0-60)	0	0
Tiva Canyon Member, Paintbrush Tuff	18.3-30.5 (60-100)	0	0
Yucca Mountain Member, Paintbrush Tuff	30.5-38.1 (100-125)	0	0
Pah Canyon Member, Paintbrush Tuff	38.1-71.6 (125-235)	0	0
Topopah Springs Member, Paintbrush Tuff	71.6-434.4 (235-1425)	2	17
Tuffaceous Beds of Calico Hills (Informal)	434.4-549.3 (1425-1802)	2	13
Prow Pass Member, Crater Flat Tuff	549.3-662.3 (1802-2173)	2	21
Bullfrog Member, Crater Flat Tuff	662.3-804.4 (2173-2639)	13	51
Tram Member, Crater Flat Tuff (Informal)	804.4-1084.5 (2639-3558)	6	45

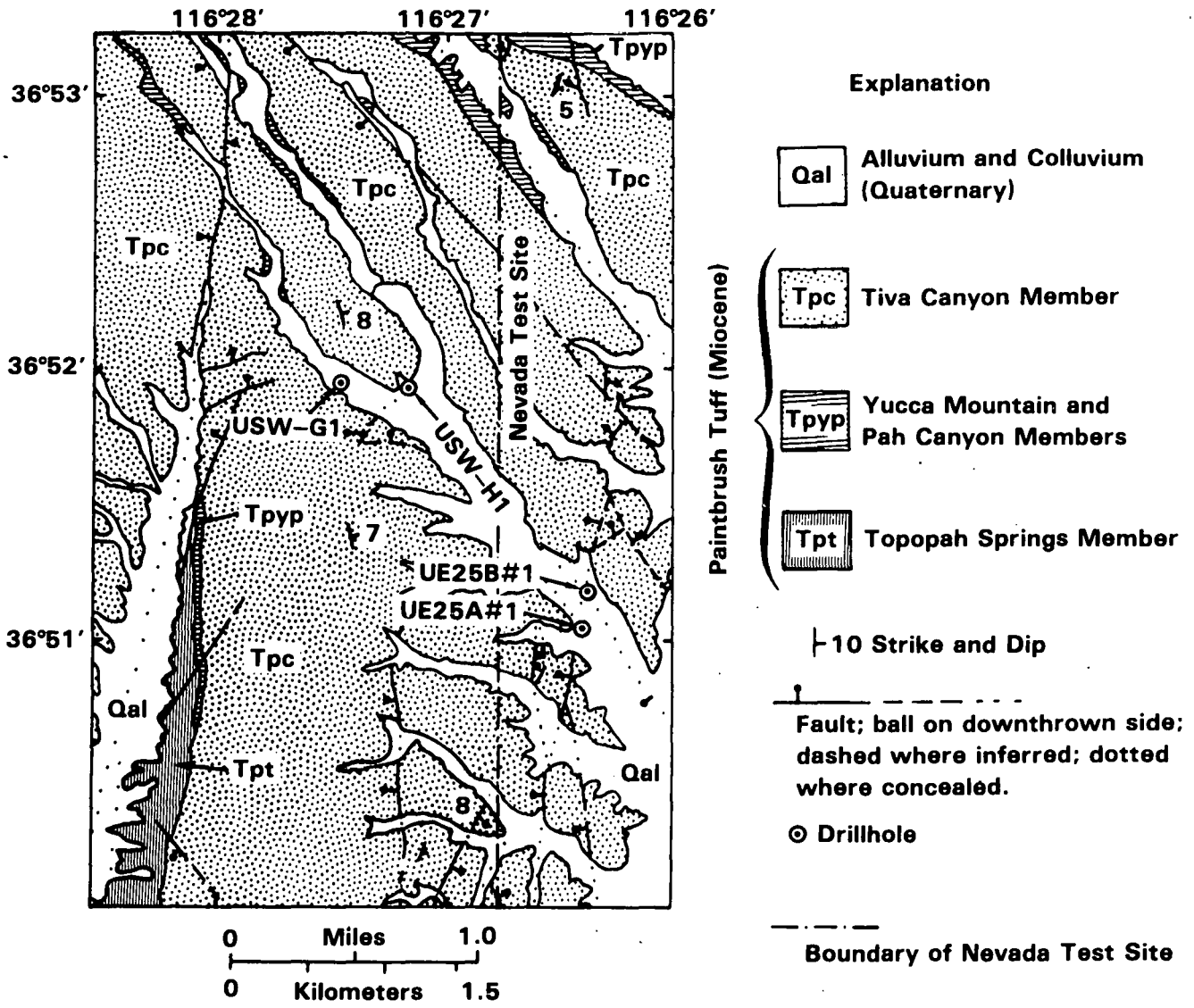

Figure 1. Index Map of Region Near Hole USW-G1 (Simplified from Reference 2)

Thermal-Conductivity Measurements

Thermal conductivities in this program were measured by a transient-line-source technique,[3] selected because of its simple application in a pressure-temperature environment. Experimental setup, data analysis, calibration, potential problems, and criteria for data acceptance are discussed in Appendix B.

Frequent calibration with fused silica at both Terra Tek and other laboratories indicates that the experimental rig used here is generally capable of measuring conductivities of uniform material having a nominal conductivity of 1 to 2 W/m°C to within ±0.06 W/m°C or less. Near the boiling of water, however, anomalously high apparent conductivities are measured (see Appendix B). Due to inherent material variability, measurements on tuff are not as precise or accurate as on the standard. Assumption of accuracy to within ±10% appears conservative.

Thermal conductivities were measured at approximately the temperatures, hydrostatic confining pressures, and fluid pressures outlined in Table 2. The room-temperature, nonpressurized tests were included for comparison and to check for possible confining-pressure effects. Subsequent testing was performed at constant confining and fluid pressure, at increasing temperatures. Fluid pressure was maintained constant at 1.5 MPa in the pressurized tests, which allowed the pore fluid to flash to steam and the sample

to dehydrate fully at ~200°C, before measurement at higher temperatures. At each test condition, duplicate measurements were generally made, with ~1/2 h allowed for the sample to stabilize between tests. If two measurements differed by > ~10%, additional measurements were made.

Test Results

Results of conductivity tests are summarized in this section in downward stratigraphic sequence, and listed in Table 3. Detailed results of each test are given in Appendix C. All bulk-property measurements made to date in each stratigraphic unit are given in Appendix D.

Table 2. Approximate Thermal-Conductivity Test Conditions

T(°C)	$P_{confining}$ (MPa)	P_{fluid} (MPa)
23	(Atmospheric)	(Atmospheric)
23	10	1.5
100	10	1.5
165	10	1.5
240	10	1.5
270	10	1.5

Table 3. Summary of Thermal-Conductivity Test Results, Upper Portion of USW-G1*

Sample Number (equivalent to depth in feet)	Grain Density (g/cm³)	Porosity	Thermal Conductivity (W/m°C) at Temperature (°C)				
			23	100	165	212	260
795.0	2.52	0.11	2.15	2.15	2.05	–	–
1330.0	2.38	0.03	1.18	1.24	1.28	1.28	1.33
1503.0	2.48	0.38	1.30	1.34	1.28	0.97	1.02
1706.0	2.33	0.33	1.17	1.21	1.24	–	–
2010.0	2.40	0.28	1.28	1.38	1.42	–	0.92
2070.0	2.41	0.29	1.33	1.43	1.47	0.97	0.91
2274.4	2.36	0.34	1.37	1.41	1.42	1.09	–
2310.0	2.44	0.37	1.38	1.43	1.43	1.80	1.05
2311.0	2.41	0.36	1.38	1.44	1.44	1.01	0.96
2367.9A	2.59	0.25	1.88	1.84	1.79	1.12	1.09
2472.3	2.62	0.32	1.88	1.84	1.85	1.14	1.15
2473.1	2.62	0.29	1.79	1.74	1.76	1.05	1.03
2474.0	2.62	0.31	1.72	1.70	1.69	1.06	1.04
2493.0B	2.62	0.27	1.88	1.90	1.93	1.15	1.17
2536.0	2.65	0.22	1.90	1.85	1.84	1.34	1.31
2568.0	2.41	0.30	1.35	1.41	1.47	1.06	1.03
2569.0	2.44	0.32	1.37	1.42	1.44	1.19	1.15
2701.0	2.42	0.31	1.39	1.44	1.45	1.20	1.02
2814.0	2.63	0.24	2.26	2.24	2.12	–	1.40
2928.3	2.65	0.19	2.07	2.02	2.01	1.55	1.52
2938.8	2.64	0.18	2.10	2.09	2.08	1.57	1.56
3050.0	2.59	0.26	1.95	1.98	1.98	–	1.53

*Tests at elevated temperature conducted at P_c = 10 MPa, P_f = 1.5 MPa. Tests at ambient temperature include both confined and unconfined results. Conductivities listed are average values for each sample at specified condition.

Topopah Spring Member, Paintbrush Tuff

The Topopah Spring Member of the Paintbrush Tuff extends between depths of 71.6 and 434.4 m (235 and 1425 ft) in Hole G1 (Table 1). The bulk of this unit, described regionally by Lipman, Christiansen, and O'Connor,[4] is densely welded and devitrified, consisting of a mix of alkali feldspar, cristobalite, and quartz.[1,4,5,6] Bulk-property measurements on this unit in Hole G1 (listed in Table D-1) indicate that matrix porosity in the central welded, devitrified zone is 0.10 to 0.12. In this study, thermal conductivity of densely welded, devitrified Topopah was measured on Sample 795 from 795 ft (242.3 m) depth. Throughout the report, sample numbers correspond to depth in feet, since all records of drilling and coring operations are kept in English units. The margins of the Topopah Springs consist of densely welded to nonwelded vitric tuffs. Sample 1330 is from the densely welded basal vitrophyre.

One complication in interpretation and application of material-property and thermal-conductivity data from the densely welded, devitrified Topopah Springs is the widespread occurrence of lithophysae in the unit. These features, originally gas-filled voids, are now lined or filled with high- and/or low-temperature minerals, and occur in locally varying concentrations throughout most of the devitrified zone. The thermal conductivity of Sample 795, which is free of lithophysae, thus cannot be applied directly to lithophysal zones.

The results of thermal-conductivity measurements on Samples 795 and 1330 are summarized in Table 3, and listed in detail in Table C-1. The fully saturated conductivity of Sample 795 (ρ_g = 2.52 g/cm^3, ϕ = 0.11) is near 2.15 W/m°C to a temperature near 100°C independent of pressure, but decreases slightly with increasing temperature, to 2.05 W/m°C (corrected, see Appendix B) at about 165°C. Measurements after dehydration, which occurs near 200°C under the confined conditions, were not successful. The confined saturated conductivity of Sample 1330 (ρ_g = 2.38 g/cm^3, ϕ = 0.03) increases from 1.18 W/m°C at ambient temperature to 1.28 W/m°C at 165°C. Dehydration has little effect, with conductivity reaching a maximum of 1.33 W/m°C at 280°C.

Saturated results on Sample 795 are in excellent agreement with previous measurements on samples from the devitrified portion of this unit. Measurements on a sample from a depth of 379.5 m (1245 ft) in Hole G1 indicate a fully saturated conductivity of 2.17 W/m°C.[7] A sample from a similar portion of this unit in Hole UE25A#1, at a depth of 481.9 m (1253 ft), has a saturated conductivity of 2.08 W/m°C.[8]

Few reliable data exist on the dehydrated thermal conductivity of this type of tuff. The reported dehydrated conductivity of Sample 1245 (unconfined) is 1.87 ± 0.04 W/m°C at temperatures between ambient and 100°C, after dehydration at near-ambient temperatures.[7] In the case of Sample UE25A#1-1253, measurements at ambient temperature after sample dehydration indicate a conductivity of 1.85 W/m°C; this decreases to 1.57 W/m°C at 100°C, and 1.40 W/m°C at 300°C. Measured conductivities on dehydrated material from the nonlithophysal, densely welded, devitrified Topopah Springs thus range from 1.85 to 1.60 W/m°C at 100°C.

A gradual increase in conductivity with increasing temperature is characteristic of many glasses. Consistent with this, Sample 1330 is from a zone that is almost entirely glassy.[4,6] In fact, the confined conductivity of 1330 after dehydration is "identical" to that reported in the literature for obsidian (1.26, 1.42 W/m°C), fused silica (1.33 to 1.36 W/m°C), and basaltic glasses (1.37 W/m°C).[9] The porosity of Sample 1330 (ϕ = 0.03) is so low that the increase in glass conductivity with increasing temperature more than makes up for any decrease in total conductivity resulting from dehydration near 200°C.

Tuffaceous Beds of Calico Hills (Informal)

The Tuffaceous Beds of Calico Hills extend from 434.4 m (1425 ft) to 549.3 m (1802 ft) in Hole G1. The unit is variable, and contains both nonwelded ashflows and bedded or reworked tuffs. Individual ashflows in the unit are nonwelded, and, as shown in Table D-2, generally characterized by high porosities (>30%) and grain densities of <2.5 g/cm^3. The low grain densities reflect extensive formation of zeolites, especially clinoptilolite.[6] The zone of zeolitization extends both upward into the lower portion of the Topopah Springs and downward into the underlying Prow Pass Member of the Crater Flat Tuff.

Thermal conductivity of two samples of nonwelded ashflow from the Tuffaceous Beds of Calico Hills was measured in this study: Samples 1503 and 1706. Results are summarized in Table 3; detailed values are given in Table C-2. In both cases, the saturated thermal conductivity is relatively constant from ambient temperature to 165°C (confined). The conductivity of Sample 1706 (ρ_g = 2.33 g/cm^3, ϕ = 0.33) increases slightly from 1.17 to 1.24 W/m°C before dehydration; that of Sample 1503 (ρ_g = 2.48 g/cm^3, ϕ = 0.38) is less temperature-dependent, remaining near 1.30 W/m°C.

The saturated conductivities from the Tuffaceous Beds of Calico Hills reported here are in good agreement with results obtained previously. Reported ambient-pressure conductivities from the unit in Hole UE25A#1 are 1.26 W/m°C at 478.2 m (1569 ft),[7] and 1.10 W/m°C at 474.0 m (1555 ft).[10] It thus appears that the saturated thermal conductivity of the ashflow portions of the Tuffaceous Beds of Calico Hills ranges only from about 1.1 to 1.35 W/m°C in Holes UE25A#1 and G1.

Measurements of dehydrated conductivity of Sample 1706 were not successful. A portion of the measurements on Sample 1503 in the dehydrated state were successful and indicate a conductivity near 1.0 W/m°C. This compares with previously reported values from Hole UE25A#1, 0.75 W/m°C at both 474.0 and 478.2 m (1555 and 1569 ft).

Prow Pass Member of the Crater Flat Tuff

The Prow Pass is the uppermost member of the Crater Flat Tuff,[11] extending between depths of 549.3 and 662.3 m (1802 and 2173 ft) in Hole G1, and between 559.6 and 711.1 m (1836 and 2333 ft) in Hole UE25A#1. The static water level, at 564-m depth, is in the upper Prow Pass in Hole G1. In this hole, the unit contains partially to moderately welded ashflow tuffs, with a thin zone of bedded/reworked tuffs at the base. Bulk-property measurements in Table D-3 indicate that porosity in the unit as a whole ranges from about 0.22 to 0.37. Grain densities, except for Samples 1886 through 1973.7, all are <2.5 g/cm^3, indicating that the bulk of the unit is zeolitized, consistent with mineralogical results.[6]

Thermal conductivity of two samples from the Prow Pass has been measured in this study: Samples 2010 and 2070. Both samples come from a partially welded, zeolitized zone. Detailed conductivity results are given in Table C-3. The apparent thermal conductivity of Sample 2010 ($\rho_g = 2.40$ g/cm^3, $\phi = 0.28$) is strongly sensitive to confining and/or fluid pressure. This response is probably caused by collapse of the sample on loading, which removed a contact resistance present at ambient pressure. The ambient-pressure data are suspect. Thermal conductivity under pressure, as shown in Table 3, increases from 1.28 to 1.42 W/m°C between ambient temperature and 165°C, and apparently decreases only slightly upon dehydration.

Given previous results,[9] the slight decrease on dehydration appears unlikely in a material of this porosity. The sample probably failed to dehydrate in the time initially allowed; only the conductivity measured at 280°C, 0.92 W/m°C, is assumed representative of the dried material.

These interpretations are supportd by results on Sample 2070. The saturated conductivity of this sample ($\rho_g = 2.41$ g/cm^3, $\phi = 0.29$) increases from 1.33 to 1.47 W/m°C between ambient temperature and 165°C, is independent of confining pressure, and decreases in a single step to 1.0 W/m°C upon dehydration near 200°C. Conductivity decreases slightly with increasing temperature above 212°C.

Samples of the Prow Pass from Hole UE25A#1 are quite different from those analyzed here. Samples at depths of 594.1, 599.2, and 609.6 m (1949, 1966, and 2000 ft) have been tested.[7 8 10] Grain densities and porosities of these three samples are 2.63 gm/cm^3, 0.18 (Sample 1949); 2.62 gm/cm^3, 0.19 (Sample 1966); and 2.56 gm/cm^3, 0.15 (Sample 2000). Thus, the samples have both higher grain density and lower porosity than those analyzed here. Reported saturated thermal conductivities of the three samples from Hole UE25A#1 are 1.76, 1.49, and 1.43 W/m°C respectively; dehydrated values 1.35, 1.12, and 1.23 W/m°C. There is thus surprisingly little difference between the reported conductivities from the Prow Pass in Hole G1, measured on samples that are zeolite-bearing and have porosities near 0.3, and those of samples from Hole UE25A#1 that have porosities near 0.2 and higher grain densities. The thermal conductivity of the Prow Pass remains poorly understood.

Bullfrog Member of the Crater Flat Tuff

The Bullfrog is the second highest member of the Crater Flat Tuff, extending between depths of 662.3 and 804.4 m (2173 and 2639 ft) in Hole G1. Within the unit as a whole there is broad variation in bulk and grain density, as well as porosity (Table D-4). The nonzeolitized, partially-to-densely-welded portion of the unit extends between depths of ~713.2 and 776.3 m (~2340 and 2547 ft). The lower portion of this interval is the most densely welded (ϕ ~0.2), and is separated from less welded tuffs below by a sharp interface. The upper boundary of the nonzeolitized zone is somewhat arbitrary.

Mineralogical analyses[6] are consistent with this subdivision of the Bullfrog. Clinoptilolite and mordenite are abundant in the upper portion of the unit, but are absent in a sample from a depth of 706.5 m (2318 ft). Zeolites are then totally absent with increasing depth until some point between samples collected at depths of 757.7 m (2486 ft), in which they are

lacking, and 778.8 m (2555 ft), in which they make up 40% to 90% of the sample. Zeolites are abundant below this depth.

For purposes of evaluating thermal conductivity of the Bullfrog, samples are broken into two groups in this study. The first group, within which conductivity has been measured successfully on six samples, contains samples from between 713.2 and 776.3 m (2340 and 2547 ft). Porosities range from 0.20 to 0.30 and grain densities from 2.55 to 2.66 g/cm^3 (see Table D-4). The second group, in which five conductivities have been measured, contains zeolitic tuffs both above and below the zeolite-free zone. Porosities in this group range from 0.25 to 0.40, and grain densities from ~2.31 to 2.58 g/cm^3.

Conductivity results for the group of samples from the central nonzeolitized portion of the unit are given in Table C-4 and summarized in Table 4, along with selected bulk properties of the tested samples. Conductivity is relatively uniform, with the standard deviation of all measurements being 0.1 W/m°C or less at all test conditions. Fully saturated conductivities of 1.7 to 1.9 W/m°C decrease to 1.05 to 1.15 W/m°C after dehydration near 200°C. The only exception is Sample 2536 which, consistent with its having the lowest porosity of samples tested, shows the smallest decrease in thermal conductivity as a result of dehydration, from 1.84 to 1.34 W/m°C.

Test results for the zeolitized tuffs above and below the central portion of the Bullfrog are given in Table C-5 and summarized in Table 5. The average saturated conductivity of these tuffs varies between 1.35 and 1.45 W/m°C, increasing slightly with increasing temperature. Conductivity decreases to 1.0 to 1.2 W/m°C upon dehydration.

Measured conductivities of nonzeolitized welded Bullfrog from Hole UE25A#1 are summarized in Table 6. In general, both saturated and dehydrated conductivities of tuffs from A#1 are greater than of material from G1. This difference appears to be real, and to correlate with lower average porosity.

Table 4. Summary of Thermal-Conductivity Test Results, Central Nonzeolitized Portion of Bullfrog Member, Crater Flat Tuff

Sample	Grain Density (g/cm^3)	Porosity	Thermal Conductivity (W/m°C) at Temperature (°C)				
			23	100	165	212-215	260-280
2367.9A	2.59	0.25	1.88	1.84	1.79	1.12	1.09
2472.3	2.62	0.32	1.88	1.84	1.85	1.14	1.05
2473.1	2.62	0.29	1.79	1.74	1.76	1.05	1.03
2474.0	2.62	0.31	1.72	1.70	1.69	1.06	1.04
2493.0B	2.62	0.27	1.88	1.90	1.93	1.15	1.17
2536.0	2.65	0.22	1.90	1.85	1.84	1.34	1.31
Average (all)	2.62	0.28	1.84	1.81	1.81	1.14	1.13
1 Standard Deviation	0.02	0.02	0.07	0.08	0.08	0.10	0.10

Table 5. Summary of Thermal-Conductivity Test Results, Zeolitized Portion of Bullfrog Member, Crater Flat Tuff

Sample	Grain Density (g/cm^3)	Porosity	Thermal Conductivity (W/m°C) at Temperature (°C)				
			23	100	165	212-215	260
2274.4	2.36	0.34	1.37	1.41	1.42	1.09	–
2310.0	2.44	0.37	1.38	1.43	1.43	1.08	1.05
2311.0	2.41	0.36	1.38	1.44	1.44	1.01	0.96
2568.0	2.41	0.30	1.35	1.41	1.47	1.06	1.03
2569.0	2.44	0.32	1.37	1.42	1.44	1.19	1.15
Average (all)	2.41	0.34	1.37	1.42	1.44	1.09	1.05
1 Standard Deviation	0.03	0.03	0.01	0.01	0.02	0.07	0.08

Table 6. Thermal-Conductivity Test Results, Bullfrog Member, Crater Flat Tuff, Hole UE25A#1 (Data from Refs 7 and 9)

Sample	Porosity	Grain Density (g/cm^3)	Approximate Thermal Conductivity (W/m°C)	
			Saturated	Dry
2341.0	0.26	2.70	–	1.74
2365.0	0.24	2.66	2.40	–
2389.0	0.25	2.61	1.47	1.06
2429.0	0.15	2.63	1.76	1.34
2432.0	0.18	2.64	2.19	1.36
2448.0	0.24	2.68	2.65	–
2499.0	0.20	2.63	1.90	1.23
Average (all)	0.22	2.65	2.06	1.35
1 Standard Deviation	0.04	0.03	0.43	0.25

Tram Member of the Crater Flat Tuff (Informal)

The Tram is the lowermost member of the Crater Flat. While the distributions of the Prow Pass and Bullfrog Members are fairly well known, very little is know about the Tram because its outcrop is limited. The member extends between depths of 804.4 and 1084.5 m (2639 and 3558 ft) in Hole G1. Mineralogical studies[6] indicate that, except for a zone extending from ~845.8 to between 914.4 and 929.7 m (~2775 to between 3000 and 3050 ft), the unit is zeolitized. In contrast to shallower zones, analcime is an important zeolite, occurring, instead of mordenite, with clinoptilolite.

Thermal conductivity has been measured on six samples from the Tram. Sample 2701, from the upper portion of the unit, is zeolitized. Samples 2814, 2842, 2928, and 2939 are from the portion free of zeolites. Sample 3050, though slightly lower in grain density than the samples above it, is considered to be within the nonzeolitized portion of the unit.

Test results for the nonzeolitized portion of the unit are given in Table C-6 and summarized in Table 7. Bulk properties for the unit are given in Table D-5. The conductivity of samples from the nonzeolitized portion is fairly uniform at between 2.0 and 2.25 W/m°C before dehydration, generally decreasing slightly with increasing temperature. The conductivity in this zone after dehydration appears to

be near 1.5 W/m°C. The zeolitized Sample (2701) from the upper portion of the Tram is similar in both conductivity and material properties to zeolitized tuffs from the Bullfrog (see Table 3).

A check of the accuracy of measurements made as part of this study is provided by data shown in Table 8. Samples at two depths within the nonzeolitized part of the Tram were split, one half analyzed at Terra Tek, the second half at the US Geological Survey laboratories in Menlo Park, California. The USGS samples were analyzed in the as-received state of saturation. As shown, there is excellent agreement between results at a depth near 892.5 m (2928 ft). The difference between the reported conductivities is only ±3% of the average value. At a depth of 895.8 m (2939 ft), the relative difference is somewhat greater, about ±8% of the average. These measurements are thus consistent with the conclusion that conductivities reported here should, conservatively, be precise to ±10%.

Table 7. Summary of Reliable Thermal-Conductivity Test Results, Nonzeolitized Portion of Tram Member, Crater Flat Tuff

Sample	Grain Density (g/cm^3)	Porosity	Thermal Conductivity (W/m°C) at Temperature (°C)				
			23	100	165	~212	245-280
2814.0	2.63	0.24	2.26	2.24	2.12	–	1.40
2928.3	2.65	0.19	2.07	2.02	2.01	1.55	1.52
2938.8	2.64	0.18	2.10	2.09	2.08	1.57	1.56
3050.0	2.59	0.26	1.95	1.98	1.98	–	1.53
Average (all)	2.63	0.22	2.10	2.08	2.05	1.56	1.50
1 Standard Deviation	0.03	0.03	0.13	0.11	0.06	–	0.07

Table 8. USGS – Terra Tek Thermal-Conductivity Comparison Test Results*

Sample Depth (ft(m))	Porosity	Grain Density (g/cm^3)	Saturated Conductivity (W/m°C)	$\Delta^{relative}$** (W/m°C)
2928.1 (892.5) (Terra Tek)	0.19	2.65	2.03	+ 0.06
2929.1 (892.8) (USGS)	0.15†	2.65	1.88(1)	– 0.09
			1.94(2)	– 0.03
2938.8 (895.8) (Terra Tek)	0.18	2.64	2.08	+ 0.12
2939.3 (895.9) (USGS)	0.16†	2.64	1.81(1)	– 0.15
			1.87(2)	– 0.09

*USGS data contained in personal communication by J. Sass, USGS, to A. R. Lappin, Sandia, dtd March 9, 1981.

**Calculated relative to the average of the Terra Tek determination and average USGS determination.

†USGS determination. All other bulk-property data from Terra Tek.

(1)Conductivity determined on disk by guarded-end-plate technique.

(2)Conductivity determined by back calculation from experimental measurement in water-filled chamber containing rubbled sample. Technique described in Ref 13.

Thermal Stratigraphy

Two factors inhibit lateral and vertical correlation of tuff thermal conductivities. First, ashflow units are inherently variable in vertical profile, especially as regards porosity. Second, as a response to variations in permeability, initial temperature, and geologic setting, tuff mineralogy varies. Any attempt at a generalized understanding of the thermal conductivity of tuffs must take both factors into account.

Correction for the effects of porosity is relatively straightforward under some conditions. Several methods have been proposed and used to back-calculate to "zero-porosity" or matrix thermal conductivity (K_o) from laboratory measurements (for example, Refs 12, 13, and 14). The method used here is an extension of that used by Woodside and Messmer.[14] In this empirical method,[9] the measured thermal conductivity, K_{rock}^{meas}, is assumed to be

$$K_{rock}^{meas} = K_o^{(1-\phi)} K_g^{\phi(1-s)} K_w^{\phi s} \quad , \tag{1}$$

where

K_{rock}^{meas} = measured rock conductivity
K_o = theoretical matrix conductivity at zero porosity
ϕ = porosity
K_g = conductivity of air
s = relative saturation of sample
K_w = conductivity of liquid water. All conductivities are in units of W/m°C, and both porosity and saturation are in decimal notation rather than percent.

By means of simple rearrangement, calculated K_o values can be obtained from

$$K_o = \left(\frac{K_{rock}^{meas}}{K_g^{\phi(1-s)} K_w^{\phi s}} \right)^{\frac{1}{(1-\phi)}} \quad . \tag{2}$$

Calculated K_o values for the samples analyzed here are given in Table 9. Because of uncertainties regarding the effective thermal conductivity of air in these samples and lack of success in previous attempts to measure conductivity of partially saturated material, the K_o values given are based on measurements at complete saturation (s = 1.0), assuming a liquid water conductivity of 0.605 W/m°C.[15] The geometric-means approach, though empirical, yields excellent agreement with other methods in calculating the matrix conductivity of basalts.[13]

Once the calculated value of the matrix thermal conductivity has been determined from measurements on fully saturated material, the conductivity of air can be calculated from measurements on fully dewatered samples. Calculated air conductivities are included in Table 9. As shown, the values fall into two distinct groups. For devitrified samples (grain density ≥ 2.5 g/cm^3), the apparent air conductivities range from 0.08 to 0.24 W/m°C, and average 0.12 ± 0.05 W/m°C. Effective air conductivities in the zeolitized tuffs range from 0.18 to 0.37 W/m°C and average 0.27 ± 0.06 W/m°C. The apparent conductivity of air in Sample 1330 is 19.66 W/m°C. These values compare with 0.03 to 0.04 W/m°C for air and steam in the same temperature and pressure range as measurements were made here.[16]

The difference between apparent and textbook values may be due to several causes. First, it is assumed here that the matrix conductivity is independent of temperature. This is almost certainly not the case.[9] In the case of devitrified tuffs, while the conductivity of feldspars may increase slightly with increasing temperature, that of quartz is well documented to decrease. Many of the samples of devitrified tuff analyzed here show a slight decrease in saturatd conductivity with increasing temperature. There is no major phase in these tuffs that should show an increase in conductivity due to dehydration, since none of the main silicate phases are dehydrated at the temperatures of interest.

A relatively high apparent thermal conductivity of air is common, however, in other studies on rocks containing primarily anhydrous phases (see, for example Ref 13), and may be due to the formalisms used, to reported porosities being slightly too high, or to heat transfer processes being active that are not included in the calculations. In the case of vesicular basalts, the apparent air thermal conductivity in dehydrated samples is 0.14 W/m°C,[13] quite close to that calculated here for devitrified tuffs, 0.12 W/m°C. Due to its apparent validity for both basalts and devitrified tuffs, this number is considered reliable.

As shown in Table 9 however, the average apparent thermal conductivity of air in dehydrated samples of zeolitized tuffs (grain density <2.5 g/cm^3) is greater than that in devitrified samples, 0.27 ± 0.06 W/m°C, vs 0.12 ± 0.05 W/m°C. Even accepting the high air conductivity in devitrified tuffs and basalts, there must be one or more additional mechanisms operating in the zeolitized samples. One factor is probably the fact that, contrary to assumptions made here, the matrix conductivity of zeolitized (and vitric) materials

actually increases with increasing temperature, especially if dehydration occurs. The effect is most striking in Sample 1330. In this case, due to the low porosity (ϕ = 0.03), the increase in glass conductivity with increasing temperature and dehydration more than makes up for the effects of dewatering, with the result that overall sample conductivity is actually highest after dehydration. The apparent air thermal conductivity after dehydration of this sample, assuming the matrix conductivity to be temperature independent at 1.20 W/m°C, is 19.66 W/m°C. If, however, it is assumed that dehydration increases the matrix conductivity of the glass in Sample 1330 to near that of anhydrous glass, say 1.4 W/m°C, then the apparent air thermal conductivity is reduced to 0.14 W/m°C, consistent with results on devitrified tuffs.

Table 9. Calculated Matrix Conductivity (K_o) and Air Thermal-Conductivity (K_g) in Analyzed Samples

Sample Number (equivalent to depth in feet)	Grain Density (g/cm^3)	Porosity	K_o(W/m°C)(1)	K_g(W/m°C)(2)
795.0	2.52	0.11	2.51	–
1330.0	2.38	0.03	1.20	19.66
1503.0	2.48	0.38	2.08	0.30
1706.0	2.33	0.33	1.62	–
2010.0	2.40	0.28	1.71	0.19
2070.0	2.41	0.29	1.83	0.18
2274.4	2.36	0.34	2.09	0.31
2310.0	2.44	0.37	2.24	0.30
2311.0	2.41	0.36	2.19	0.24
2367.9A	2.59	0.25	2.74	0.07
2472.3	2.62	0.32	3.21	0.13
2473.1	2.62	0.29	2.79	0.09
2474.0	2.62	0.31	2.75	0.12
2493.0B	2.62	0.27	2.86	0.10
2536.0	2.65	0.22	2.62	0.12
2568.0	2.41	0.30	1.90	0.26
2569.0	2.44	0.32	2.01	0.37
2701.0	2.42	0.31	2.02	0.29
2814.0	2.63	0.24	3.43	0.08
2928.3	2.65	0.19	2.76	0.13
2938.8	2.64	0.18	2.76	0.12
3050.0	2.59	0.26	2.94	0.24

(1) $K_o = \left(\frac{K_{meas}^{s-1}}{(K_{water})^{\phi}}\right)^{\frac{1}{(1-\phi)}}$, where K_{meas} is measured in the fully saturated state, and K_{water} taken to be 0.605 W/m°C (Ref 15)

(2) $K_g = \left(\frac{K_{meas}^{s-0}}{K_o^{(1-\phi)}}\right)^{\frac{1}{\phi}}$, where K_{meas} is measured in the dehydrated state, and K_o is calculated as defined above.

A similar argument can be made with partial success in the case of zeolitized tuffs. Conductivities of dehydrated zeolites (in addition to opal and expandable clays) are unknown. Several of the zeolitized samples analyzed here show a slight increase in thermal conductivity in the saturated state with increasing temperature. The average matrix conductivity of these tuffs in the saturated state is 1.97 W/m°C. If it is assumed that the effective thermal conductivity of air in the dewatered samples is 0.12 W/m°C, then, at the average porosity of 0.33, a dehydrated thermal conductivity of 1.04 W/m°C requires a matrix conductivity of 3.01 W/m°C, as opposed to the assumed value of 1.97 W/m°C. This appears unlikely. Another possibility, since water is released from such hydrous phases as zeolites over a range of temperatures, is that the transient heating of a portion of these tuffs during conductivity measurement in the "dehydrated" condition results in vaporization of additional crystal-bound water near the heating probe. Such a process would be endothermic, and result in too high an apparent thermal conductivity.

The prediction of thermal conductivity of dehydrated, zeolitized tuffs is thus somewhat unsatisfactory using the geometric-means approach, since it requires use of an effective air conductivity of 0.27 W/m°C, an order of magnitude greater than the textbook value. However, so long as the porosity range to which estimated conductivities are extrapolated is similar to that from which the zero-porosity conductivities were calculated, the results should be reliable. In the case of zeolitized tuffs, results would appear reliable for tuffs having porosities between ~0.25 and 0.40.

Variations in zero-porosity or matrix conductivity as a function of mineralogy can, to a first approximation, be understood as a function of grain density. This is helpful in extrapolation of conductivities to regions where mineralogical data are not available. Lappin[9] developed a theoretical curve of K_o vs grain density, and related this curve to both mineralogy and early experimental results. The theoretical curve, results reported here, and some earlier experimental results are shown in Figure 2.

In Figure 2, Curve A represents approximate changes in grain density and matrix conductivity resulting from zeolite formation at the expense of primary anhydrous glass having a density of 2.41 g/cm^3 and conductivity of 1.35 W/m°C.[9] There is little apparent change in thermal conductivity because of zeolitization, though conductivity data for zeolites are sparse; none are available for clinoptilolite. Hydration of initially anhydrous glass (as in the case of Sample 1330) decreases its conductivity and grain density below values shown in the figure. Curve B represents changes in both thermal conductivity and grain density as anhydrous glass devitrifies to a mix of cristobalite and alkali feldspar, assuming a 30:60 ratio of cristobalite/feldspar. Curve C represents changes in density and conductivity with varying cristobalite/feldspar ratios, assuming complete devitrification. Curve D represents variations in matrix conductivity and density in quartz-bearing tuffs, assuming complete inversion of cristobalite. Assuming that phenocrysts and secondary phases such as montmorillonitic clays are negligible, the curves in Figure 2 should provide an estimate of minimum zero-porosity thermal conductivity as a function of both grain density and mineralogy.

The relationship between grain density and mineralogy provides a method for dividing most tuffs into three distinct groups. Tuffs with a grain density $< \sim 2.5$ g/cm^3 should either be vitric or should have undergone some zeolitization (Trend A) and/or devitrification to feldspar and cristobalite (Trend B). Tuffs that have undergone a combination of zeolitization and devitrification should have a zero-porosity conductivity lying above the A and B lines, in field E. Tuffs with a grain density between 2.5 and 2.58 g/cm^3 should be simply devitrified, consisting largely of cristobalite and feldspars. Tuffs with a grain density of > 2.58 g/cm^3 should be largely a mixture of quartz and alkali feldspars.

Mineralogical studies to date,[5,6] generally support this subdivision. Eight of the 10 zeolitized tuffs studied here come from zones in which the combined total of zeolite, cristobalite, and feldspars is >90% of the rock. Clay contents are low and quartz contents <10%.[6] In most cases, the estimated content of cristobalite is also quite low, so that the tuffs may be thought of as a mix of zeolite and feldspar. The average calculated zero-porosity conductivity of the 10 zeolitized tuffs studied here is 1.97 ± 0.20 W/m°C, represented by value 1 in Figure 2. Average grain density is 2.41 ± 0.04 g/cm^3. Zero-porosity conductivity of these tuffs is thus statistically uniform within experimental error, independent of depth and stratigraphic unit.

Results for the six sets of data on the nonzeolitized portion of the Bullfrog are also quite uniform, as indicated by point 2 in Figure 2. The reported mineralogy in this portion of the unit consists of >95% total quartz, feldspars, and cristobalite (or opal).[6] The average zero-porosity conductivity of the nonzeolitized Bullfrog is 2.83 ± 0.20 W/m°C in Hole G1 (point 2, Figure 2), compared to 2.91 ± 0.89 W/m°C in Hole A#1 (point 3). Average grain densities are 2.62 ± 0.03 and 2.65 ± 0.03 g/cm^3, respectively. Thus, although the

measured saturated conductivities are somewhat different, there is no statistically significant difference between the average zero-porosity thermal conductivities of the nonzeolitized Bullfrog in the two holes. Zero-porosity conductivity (2.97 ± 0.32 W/m°C; point 4, Figure 2) and average grain density (2.63 ± 0.03 g/cm^3) of nonzeolitized samples from the Tram are almost identical to corresponding values for the Bullfrog in both Hole G1 and Hole A#1.

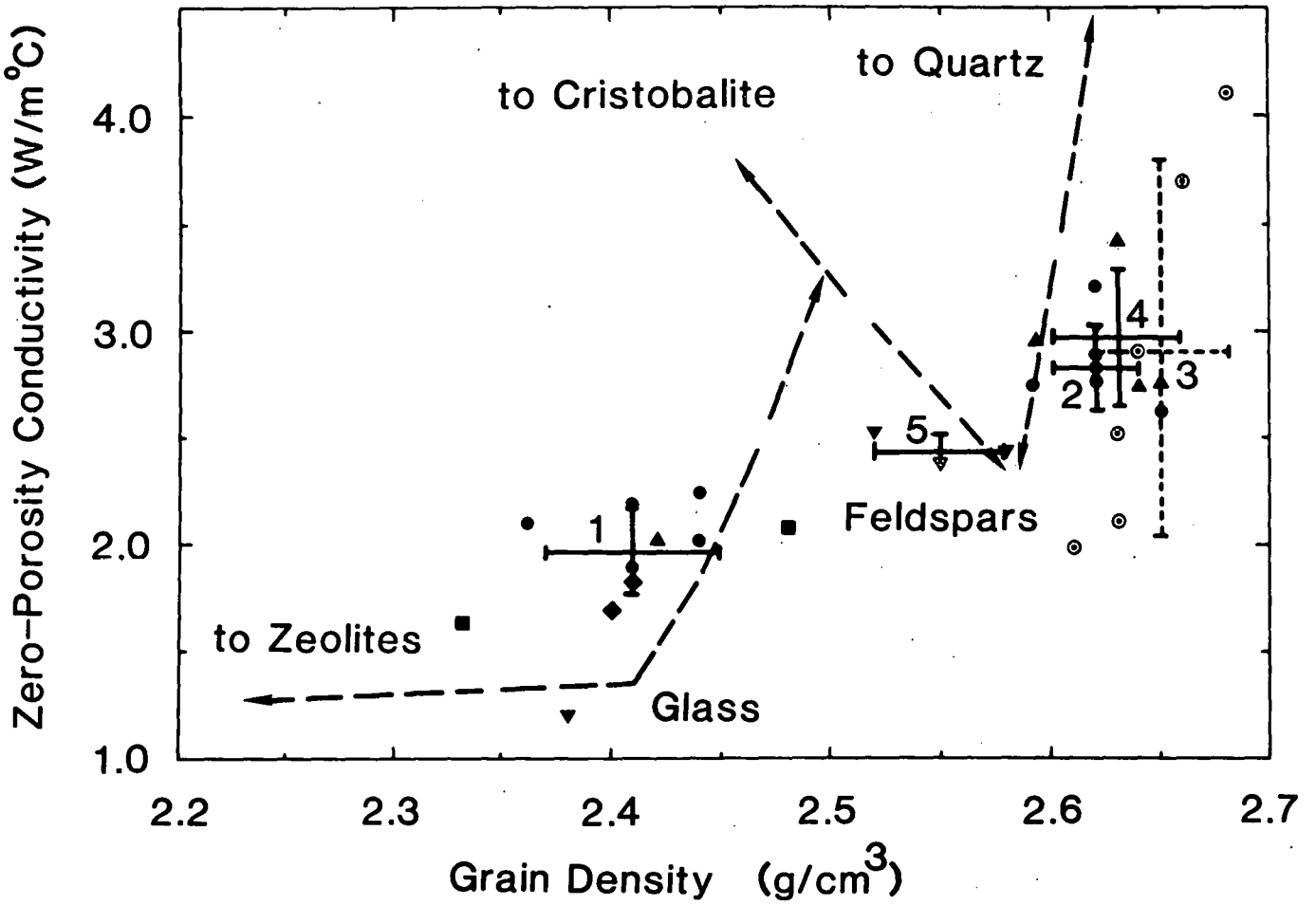

Legend

Unit	Hole	Symbols	Unit	Hole	Symbols
Topopah Springs Member, Paintbrush Tuff	G1 A1	▼ ▽	All Zeolitized Tuffs (Average K_o, ρ_g)	G1	1
Tuffaceous Beds of Calico Hills	G1 A1	■ ⊡	Nonzeolitized Bullfrog (Average K_o, ρ_g)	G1 A1	2 3
Prow Pass Member, Crater Flatt Tuff	G1 A1	◆ ◇	Nonzeolitized Tram (Average K_o, ρ_g)	G1	4
Bulldog Member, Crater Flat Tuff	G1 A1	● ⊙	Densely Welded, Devitrified Topopah Springs (Average K_o, ρ_g)	G1 A1	5
Tram Member, Crater Flat Tuff	G1	▲			

Figure 2. Theoretical Grain Density-Conductivity Relationship and Calculated K_o Values for Silicic Tuffs From UE25A#1 and USW-G1

The zero-porosity conductivity of all nonzeolitized Bullfrog and Tram samples analyzed to date averages 2.89 ± 0.53 W/m°C. The average zero-porosity conductivities of the three data sets are 2.83, 2.91, and 2.97 W/m°C. Average zero-porosity conductivities of these nonzeolitized devitrified tuffs thus appear to be statistically uniform, independent of depth, stratigraphic unit, and location. There may be some statistically significant variation within the welded Bullfrog in Hole A#1.

It should be noted that zero-porosity conductivities calculated here for devitrified, welded Bullfrog and Tram, while internally consistent, are lower than expected solely on the basis of simplified mineralogy. Reported quartz/feldspar ratios in devitrified Tram and Bullfrog analyzed to date range from ~30/60 to 50/40. Ignoring the presence of all other minerals, this should lead to zero-porosity conductivities between 3.5 and 4.2 W/m°C, as compared to the average calculated value of 2.9 W/m°C. The difference may be due to either invalidity of some of the assumptions inherent in the geometric-means formalism or to effects of small amounts of such phases as expandable clays, not considered here. Nonetheless, use of the approach described here yields internally consistent results, applicable over a porosity interval similar to that of the samples from which calculated zero-porosity conductivities have been derived. On the basis of the samples analyzed here, the range of reliable application appears to extend between 0.2 and 0.4 porosity.

Data for evaluation of the densely welded, devitrified Topopah Springs are limited. Three measurements of saturated conductivity in this zone lead to a calculated zero-porosity conductivity of 2.44 ± 0.08 W/m°C, shown as Point 5 in Figure 2. Average grain density of these samples is 2.55 ± 0.03 g/cm^3. Note that, though Samples 795 and 1245 both come from zones in which there has been only limited inversion of cristobalite to quartz, abundant quartz does occur locally within devitrified portions of the Topopah Springs.[5,6] Although the data are extremely limited, it is tentatively concluded that zero-porosity conductivity of cristobalite-bearing devitrified welded tuffs with grain densities between ~2.5 and 2.58 g/cm^3 is also statistically uniform, indpendent of location.

When combined with the bulk-property measurements given in Appendix D, the conductivity results presented here provide a basis for developing a saturated thermal-conductivity stratigraphy for intact materials in the upper portion of Hole G1. In all units but the Topopah Springs, it is assumed that reported values are representative of the units sampled in the absence of fractures. In the case of the Topopah Springs, correction must be made for the occurrence of lithophysal cavities and incomplete matrix saturation.

With the exception of zeolitized tuffs, estimation of the potential effects of in-situ joints is relatively straightforward. Preliminary measurements indicate that a linear thermal expansion coefficient of 10×10^{-6}°C^{-1} is reasonable for devitrified tuffs both above and below the water table.[17] Assuming this to be true, that the temperature at which a welded tuff is emplaced is no greater than 1000°C[3], that all contraction during cooling is taken up in the form of planar joints, and that there is no reduction in joint aperture due to overburden or tectonic stresses, a maximum of ~1% of the initial material length should be taken up by fractures at ambient temperature. This would correspond to a fracture porosity of 3 vol %, and would almost certainly be an overestimate in most cases.

In the simple case of heat flow perpendicular to a set or series of planar joints, the effective thermal conductivity of the jointed mass (K_{eff}) is given by the relation shown in Equation 3, where K_i and X_i are respectively taken as the conductivity and length fraction occupied by the intact material, and K_j and X_j the corresponding values for the joints. In the cases for welded tuff considered here, K_j is taken to be either 0.605 or 0.12 W/m°C, depending upon whether the joints are assumed to be water or air-filled. X_i and X_j are 0.99 and 0.01 in all cases, corresponding to 3% fracture porosity.

$$K_{eff} = \frac{1}{\frac{X_i}{K_i} + \frac{X_j}{K_j}} \quad . \tag{3}$$

The effects of estimated maximum fracture porosities on the in-situ thermal conductivity of devitrified welded tuffs are shown in Table 10. In the case of saturated tuffs below the water table, the estimated reduction in in-situ conductivity is well below 10%, and is considered negligible. If these tuffs are assumed to be dehydrated, however, including the contained joints, the effect is on the order of 10%, but still quite minor. Thus, it is concluded that effects of inherent thermally-induced jointing on the in-situ thermal conductivity of devitrified welded tuffs below the water table are negligible.

This may not be the case in such welded tuffs as the Topopah Springs, when situated above the water table. In this setting, although the matrix may be near full saturation, virtually all joints may be assumed air-filled. Under this assumption, the ambient-temperature conductivity of nonlithophysal Topopah

may be reduced from 2.1 to 1.8 W/m°C, about 15%. A similar but smaller reduction in conductivity of the dehydrated rock mass is also possible. It is therefore concluded that in the case of the Topopah Springs, which is the most densely welded tuff encountered at Yucca Mountain, effects of natural in-situ jointing on rock-mass conductivity may need to be considered.

Potential effects of nontectonic fracturing on the in-situ thermal conductivity of zeolitized or nonwelded tuffs appear negligible. Since they are often emplaced as either ash-fall tuffs at near-ambient temperature or as marginal envelopes to ashflow sheets, such tuffs may have undergone only very limited cooling in place. Thermally-induced jointing should therefore be negligible. In addition, zeolitization of zeolitized welded tuffs may have greatly reduced any initial fracture porosity. It is thus concluded that the in-situ rock-mass thermal conductivity of heavily zeolitized or nonwelded tuffs should be quite near that of the intact material.

This is likely not the case in dehydrated zeolitic tuffs. Preliminary information indicates that zeolitized (or vitric) tuffs may contract up to 3 vol % or more upon dehydration. If a 3% figure is assumed representative, then the in-situ conductivity of zeolitized tuffs in the dehydrated state, assuming the effective conductivity of air in the joints to be 0.12 W/m°C, might be reduced from the value of 1.04 W/m°C measured on intact material to ~0.97 W/m°C. This change is probably negligible.

Table 11 contains the estimated conductivity stratigraphy for intact material from Hole USW-G1 below a depth of 409.1 m (1342 ft). Contacts between individual zones were chosen largely on the basis of bulk-property measurements and mineralogical studies. When possible, however, a combination of laboratory measurements and data from the downhole density log was used. Numbers of specimens analyzed for bulk properties in each zone, average grain densities, and average porosities are listed. The individual layers are relatively uniform internally, especially the nonzeolitized welded tuffs. Initial saturation of nonwelded zeolitized tuffs, even above the water table is near 1.0. Estimated conductivities were calculated using the geometric-means formula (Equation 1), average porosities for each zone, and zero-porosity conductivities of 1.95 W/m°C for the heavily zeolitized tuffs and 2.90 W/m°C for the nonzeolitized welded tuffs. The average of the experimental measurements generally falls within one standard deviation or less of the calculated saturated conductivity for that zone.

Table 10. Estimated Maximum Effects of In-Situ Thermal Fracturing on Rock-Mass Thermal-Conductivity of Welded Devitrified Tuffs (Excluding Lithophysal Topopah Springs)

Rock Type (Setting)	Thermal Conductivity of Intact Material (W/m°C)	Calculated Rock-Mass Conductivity[1] (W/m°C)	Δ(W/m°C)[2]	Δ%[3]
Welded Devitrified Tram (below water table)	2.10 (saturated) 1.56 (dry)	2.05 (matrix and joints saturated) 1.39 (matrix and joints dry)	0.05 0.17	2.4 10.9
Welded Devitrified Bullfrog (below water table)	1.84 (saturated) 1.14 (dry)	1.80 (matrix and joints saturated) 1.05 (matrix and joints dry)	0.04 0.09	2.2 7.9
Welded Devitrified Topopah Springs (above water table)	2.10 (saturated) 1.85 (dry)	1.80 (matrix saturated, joints dry) 1.62 (matrix and joints dry)	0.30 0.23	14.3 12.4

[1]Calculated from $K_{eff} = \frac{1}{\frac{X_i}{K_i} + \frac{X_j}{K_j}}$; symbols defined in text

[2]Thermal conductivity of intact material – calculated rock-mass conductivity

[3](Δ(W/m°C) divided by conductivity of intact material) x 100

Table 11. Estimated Thermal-Conductivity and Bulk-Property Stratigraphy (Saturated) of Upper Portion of Hole USW-G1 Below 409.1 m (1342 ft)

Depth Interval (m(ft))	Rock Type Unit	Grain Density (g/cm³)			Porosity			Saturated Thermal Conductivity (W/m°C)				Fully Dehydrated Thermal Conductivity (W/m°C)			
								Calculated[4]		Measured		Calculated[5]		Measured	
		N[1]	X[2]	1σ[3]	N	X	1σ	K	N	K	1σ	K	N	K	1σ
409.1-569.1 (1342-1867)	Zeolitized, non to partially welded	16	2.40	0.09	16	0.34	0.03	1.31	2	1.24	–	1.00	1	1.00	–
569.1-605.6 (1867-1987)	Nonzeolitized, partially to moderately welded	5	2.57	0.04	5	0.31	0.04	1.78	–	–	–	1.08	–	–	–
605.6-713.2 (1987-2340)	Zeolitized, non to partially welded	28	2.43	0.07	28	0.33	0.04	1.33	5	1.35	0.04	1.02	5	1.00	0.07
713.2-776.3 (2340-2547)	Nonzeolitized, partially to densely welded	24	2.61	0.02	26	0.26	0.03	1.87	6	1.84	0.07	1.27	6	1.14	0.10
776.3-847.4 (2547-2780)	Zeolitized, non to partially welded	19	2.43	0.06	19	0.28	0.03	1.41	3	1.37	0.02	1.12	3	1.11	0.06
847.4-920.5 (2780-3020)	Nonzeolitized, partially to moderately welded	14	2.63	0.03	13	0.20	0.03	2.12	4	2.10	0.13	1.53	4	1.51	0.07

[1]N = Number of samples analyzed

[2]X = Average of measurements on analyzed samples

[3]σ = Standard deviation

[4]$K_{sat}^{calc} = K_o^{(1-\phi)} K_w^{\phi}$; K_o values defined in text

[5]Calculated values derived from $K_{deh}^{calc} = K_o^{(1-\phi)} K_g^{\phi}$; K_o and K_g defined in text

Saturated conductivities listed in Table 11 should be fairly reliable. There is general agreement between experimental and calculated results, and no major internal structural complication in these units that might affect data interpretation. Assumption of complete initial saturation is reasonable, and changes in porosity occur over relatively short stratigraphic intervals, documented both by downhole logging and laboratory measurements. Likewise, there is good agreement between calculated and measured conductivities in the dehydrated condition, using effective air conductivities of 0.12 W/m°C in the nonzeolitized tuffs and 0.27 W/m°C in the zeolitized. The agreement between measured and calculated values indicates that the samples on which conductivity was measured are representative of the depth zones containing them.

This is not the case at depths of $< \sim$411.5 m (1350 ft), since the major unit at these depths, the Topopah Springs Member of the Paintbrush Tuff, is internally complex, and not fully saturated. As mentioned above, the unit contains abundant lithophysal cavities, which are usually partially gas-filled. Therefore, to predict the in-situ thermal conductivity of the Topopah Springs, even assuming complete matrix saturation, an estimate must be made of the effect of air-filled porosity on thermal conductivity.

The initial approach taken here is to assume that the matrix or intact material in lithophysal portions of the Topopah has a porosity of 0.10 and saturated thermal conductivity of 2.1 W/m°C. Lithophysae are then considered to have a thermal conductivity of 0.12 W/m°C. The effective conductivity of the rock mass is calculated using the geometric means approach, with the conductivity of the intact material taking the place of the zero-porosity conductivity in previous calculations.

Estimated conductivity for the Topopah Springs as a function of depth is given in Table 12, with lithophysal void volumes estimated for Spengler, et al.[1] The approximate average conductivity perpendicular to layering for the densely welded, devitrified portion of the Topopah Springs is reduced from $\sim$2.1 to $\sim$1.6 W/m°C by the presence of lithophysae in the

matrix-saturated state. Assuming 0.6 to be the matrix saturation in this zone, the conductivity is reduced slightly, the conductivity of nonlithophysal material to 2.00 W/m°C, and that of the unit as a whole (perpendicular to layering) to 1.5 W/m°C. Bracketed values listed in Table 12 assume total dehydration and affective air conductivity of 0.12 W/m°C.

An additional area of uncertainty presently remains in estimation of thermal conductivity of the tuffs in Hole G1 above the water table. Sample 1330 is the only sample analyzed to date that consists largely of glass. In the depth intervals between 9.1 and 89.3 m (30 and 293 ft), as well as between 392.3 and 424.9 m (1287 and 1394 ft), field description and mineralogical studies[1,6] indicate that the tuffs are almost entirely glassy. Bulk-property determinations in these intervals are few. One approach to estimating thermal conductivity is to assume that the zero-porosity thermal conductivity of all glassy tuffs is the same as that of Sample 1330, 1.20 W/m°C. With this assumption and the assumption that the average porosity in the two intervals is 0.30, estimated thermal conductivity in the saturated state is ~1.0 W/m°C. If 0.6 saturation is assumed, this is reduced to 0.8 W/m°C. The same range of conductivities is assumed here for near-surface alluvium.

Table 12. Estimated Thermal-Conductivity and Bulk-Property Stratigraphy (Matrix-Saturated) of Upper Portion of Hole USW-G1 Above 409.1 m (1342 ft)*

Depth Interval (m(ft))	Rock Type	Estimated Porosity or Assumption About Lithophysae	Thermal Conductivity (W/m°C)**
0-89.3 (0-293)	Alluvium, Nonwelded Vitric, Thin Densely Welded Vitric	Porosity = 0.30	1.0(0.8) [0.6]
	Densely Welded, Devitrified		
89.3-133.5 (293-438)	Vapor Phase Zone	0% Lith.(1)	2.1(2.0) [1.8]
133.5-141.1 (438-463)	10% to 30% Lith.(1)	30% Lith.	0.9(0.85) [0.80]
141.1-150.3 (463-493)	Densely Welded	0% Lith.	2.1(2.0) [1.8]
150.3-217.3 (493-713)	20% to 30% Lith., "Commonly Filled"	15% Lith.	1.4(1.3) [1.2]
217.3-248.4 (713-815)	Rare Lith., 5% to 15% Lith., Occasional Lith.	5% Lith.	1.3(1.7) [1.6]
248.4-294.8 (815-967)	5% to 20% Lith., "Generally Filled"	10% Lith.	1.6(1.5) [1.4]
294.8-303.9 (967-997)	20% to 30% Lith., "Filled"	10% Lith.	1.6(1.5) [1.4]
303.9-365.5 (997-1199)	5% to 15% Lith., "1/2 Filled, 1/2 Unfilled"	10% Lith.	1.6(1.5) [1.4]
365.5-392.3 (1199-1287)	"Occasional" Lith.	0% Lith.	2.1(2.0) [1.8]
392.3-409.1 (1287-1342)	Densely Welded to Nonwelded, Vitric	Porosity = 0.30	1.0(0.8) [0.6]

*Parenthetical values assume 0.6 matrix saturation; bracketed values assume 0.0 matrix saturation

**Matrix porosity of densely welded, devitrified tuff assumed to be 0.10

(1)Lith. = Lithophysae

Tables 11 and 12 thus provide an estimated thermal-conductivity stratigraphy in the matrix-saturated state for intact material from the upper portion of Hole G1, and for the partial-saturation state of the densely welded Topopah Springs and vitric tuffs above and below it. The tables do not consider possible effects of jointing on in-situ thermal conductivity, since these generally appear to be negligible.

Conclusions and Discussions

Test results presented here are consistent with the conclusion that it is possible to measure the thermal conductivity of most silicic tuffs to within ±10% or better using the transient-line-source technique. Zero-porosity or matrix thermal conductivity of heavily zeolitized tuffs appears statistically uniform near 1.95 W/m°C, independent of depth, stratigraphic formation, and detailed mineralogy. Zero-porosity conductivity of nonzeolitized welded tuffs appears uniform near 2.9 W/m°C, independent of formation, depth, and location. Combination of average zero-porosity conductivities and effective air conductivities of 0.12 W/m°C in devitrified tuffs and 0.27 W/m°C in zeolitized tuffs with laboratory bulk-property measurements, downhole density logs, and results of mineralogical studies allows development of a thermal-conductivity stratigraphy for intact portions of the silicic tuffs in the upper portion of Hole USW-G1 as shown in Tables 11 and 12. Calculated conductivities should be valid so long as they are for tuffs ranging generally from 0.2 to 0.4 in porosity. In the case of such tuffs as the Topopah Springs, the range of validity remains to be determined.

In the stratigraphy, individual zones, the boundaries of which do not coincide with boundaries of named stratigraphic units, are relatively uniform internally. In most cases, the standard deviations in porosity and grain density within a zone are no greater than between duplicate measurements on the same sample. Estimated conductivities of tuffs below the water table are most reliable. Above the water table, the detailed in-situ state of saturation remains unknown, and the major unit encountered, the Topopah Springs Member of the Paintbrush Tuff, is internally complex due to abundant lithophysae. At present, laboratory data are not available on the thermal conductivity of lithophysal zones. With the exception of the Topopah Springs, the values in Tables 11 and 12 should be within 10% of the in-situ thermal conductivity, based on estimated effects of thermally induced fracturing. The effect of such fracturing is greatest (~14%) in devitrified, nonlithophysal Topopah Springs above the water table.

Much obviously remains to be done. The thermal-conductivity data coverage is quite uneven; most of the emphasis to date has been placed on tuffs below the water table, especially the nonzeolitized portions of the Bullfrog and Tram Members of the Crater Flat Tuff. Below the water table, additional measurements are needed in the welded zeolitized portions of the section.

Above the water table, further characterization of the Topopah Springs is required, including measurements and confirmation of an adequate predictive model for the thermal conductivity in lithophysal zones. In addition, measurements must be made across the lower contact of the Topopah Springs, from the densely welded devitrified portion of the unit into the nonwelded vitric tuffs at its base.

Lateral extrapolation of the results and formalisms presented here involves uncertainties. As presently developed, the linking of conductivity with mineralogy is indirect. This is necessary in regions where mineralogical data are unavailable, but risky in regions near contacts between zeolitized and nonzeolitized zones. Additional mineralogy is required, especially at and near such contacts.

APPENDIX A

Test Procedures for Sample Preparation and Bulk-Property Measurements

Sample Preparation

Samples were prepared from competent sections of sealed core received from USW-G1. Water was used as a cooling medium during all cutting and coring operations.

Although theories exist to estimate thermal conductivity of partially saturated materials, successful measurements on tuff have been made to date only on fully saturated or fully dehydrated samples. Specimens were rehydrated by a vacuum-submersion technique in which the sample is placed in a container of deionized water and a vacuum drawn to the vapor pressure of water. This vacuum is sustained for 2 to 3 h, at which time the sample is removed and weighed. The evacuation and weighing process is repeated until no weight gain is observed between weighings.

As-received saturation in these tuffs is generally 0.7 to 0.9, so the only pore spaces requiring rehydration are presumably near surfaces dehydrated during handling and preparation. Thus, the connate water in the center of the core has apparently not been disturbed. The application of pore pressure during testing further reduces the amount of gas-filled void space in the core.

Bulk Properties

Bulk properties were measured by standard methods. Detailed procedures, summarized below, are on file with Sandia National Laboratories Quality Assurance.

Bulk Density

Bulk density is determined by weighing a specimen in water and measuring its volume by mercury displacement. No attempt was made here to preserve the initial state of saturation. The specimen is then oven-dried at $110 \pm 5°C$ to constant weight and reweighed. The original weight divided by the volume yields the initial bulk density. Dried weight divided by initial volume yields dry density, assuming no change in sample volume during drying. These relations are summarized:

$$\text{Bulk Density} = \frac{\text{orig. wt.}}{\text{orig. vol.}} \quad \text{Dry Density} = \frac{\text{dry wt.}}{\text{orig. vol.}}$$

Grain Density

The dried specimen is crushed, pulverized to approximately 100 mesh size, and weighed. Grain volume is measured by water immersion. Weights are accurate to $\pm 0.1\%$ and volumes to 1.0%. Grain density is found by dividing grain weight by grain volume.

$$\text{Grain Density} = \frac{\text{grain wt.}}{\text{grain vol.}}$$

Initial Water Content

The water content of the specimen is calculated by subtracting the specimen's dry weight from the initial weight and dividing the resultant by the initial weight.

$$\text{Initial Water Content} = \frac{\text{orig. wt.} - \text{dry wt.}}{\text{orig. wt.}}$$

Total Porosity

The total porosity of the specimen is calculated from the dry bulk density and grain density as follows:

$$\text{Total Porosity} = 1 - \frac{\text{Dry Density}}{\text{Grain Density}}$$

Note that the "total porosity" reported here is based on grain densities measured after crushing of the material to minus 100 mesh. Micropores completely contained in grains passing this mesh, i.e., less than

about 0.15 mm in diameter, might be occluded and not included in the porosity measurement, except as they decrease apparent grain density if dewatered during sample drying.

Saturation

Reported saturations are calculated from the relation:

$$\text{Saturation} = \frac{\text{Orig. Bulk Density} - \text{Dry Bulk Density}}{\text{Porosity}}$$

Bulk Density at Total Saturation

This value is calculated from the relation:

Bulk Density at Total Saturation =
(Grain Density x $(1 - \phi) + \phi$)

APPENDIX B

Test Procedures, Calibration, and Data-Acceptance Criteria for Thermal-Conductivity Measurements

A schematic of the thermal-conductivity test setup is shown in Figure B-1. As shown, a 0.32-cm-dia. heater approximating an ideal line source is placed along the longitudinal axis of a 5.1-cm-dia. by 10.2-cm-long sample. A thermocouple is attached and soldered to the heater at midsample. The entire probe assembly is "potted" in place with a mixture of ceramic cement and powdered copper to minimize and standardize contact resistance between probe and sample. Disks of low-conductivity ceramic insulator are used to minimize heat loss from the ends of the sample. Such heat losses, if unchecked, would lead to anomalously high apparent conductivities. The overall internal heater length, 13.4 cm, gives a heater length-to-diameter (L/D) ratio of 36. The L/D ratio within the sample itself is 32. The sample-probe assembly is separated from the confining fluid by a teflon sleeve.

Power, in the form of carefully monitored and controlled voltage and current, is applied to the probe heater for periods of <2 min, while the exterior of the sample is maintained at constant pressure and nearly constant temperature ($\Delta T < 1°C$). Because the exterior temperature of the sample does not change significantly during the period of the test, a sample of finite dimension behaves as if it were inifinite in volume.

Thermal conductivity for the material is calculated from the internal heater temperature history and power input according to

$$K = \frac{P}{4\pi\Delta T} \ln \frac{t_2}{t_1},$$

by determining the least-squares best fit to the experimental data between 30 (t_1) and 90 (t_2) s. In the equation, K is the rock thermal conductivity in W/m°C, ΔT the change in heater temperature between times t_1 and t_2, and P the heater power in W/m.

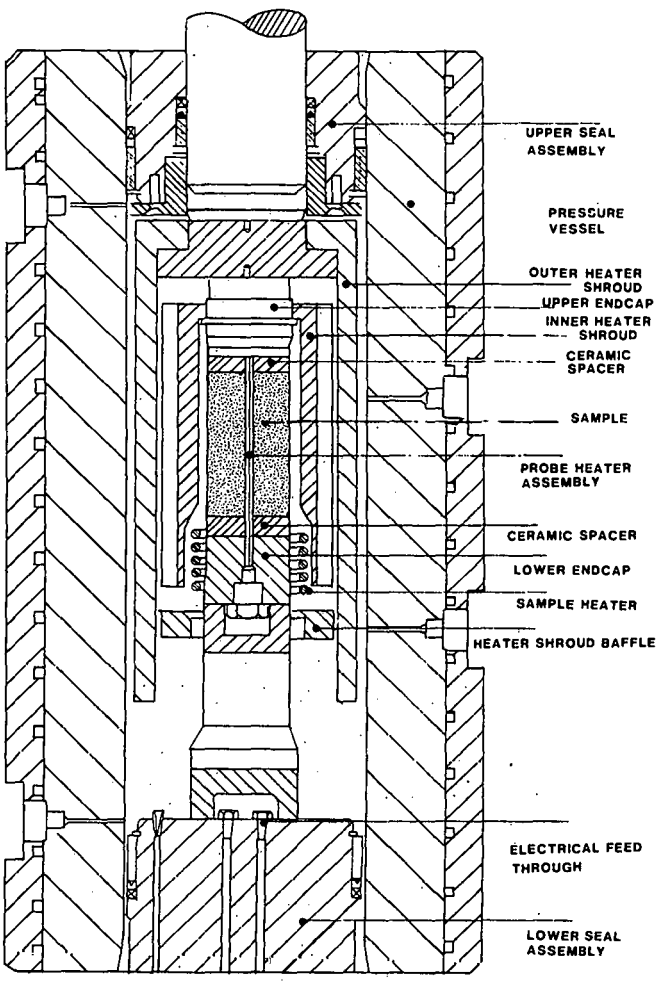

Figure B-1 Schematic of Thermal-Conductivity Test Setup

Figure B-2 is a temperature -ln(t) plot from a representative thermal-conductivity measurement. Note that the initial response of the heater is not log-linear. At longer times, beginning 20 to 30 s into the test, the response is log-linear. In Figure B-3, temperature is plotted against time on a linear time scale. This figure emphasizes the short duration of the early transient period.

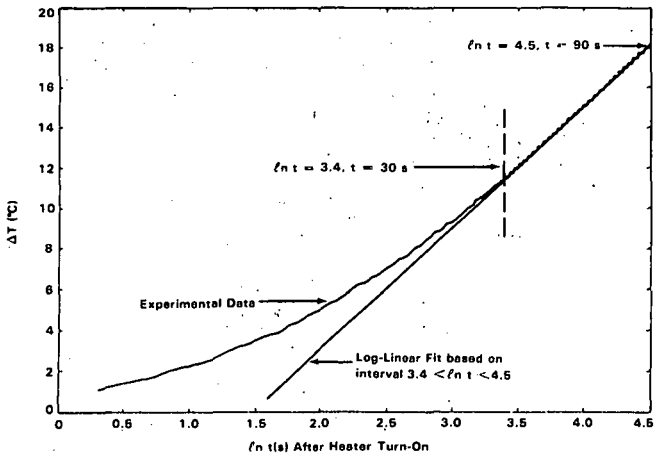

Figure B-2 ΔT-ln Time Plot, Representative Conductivity Test

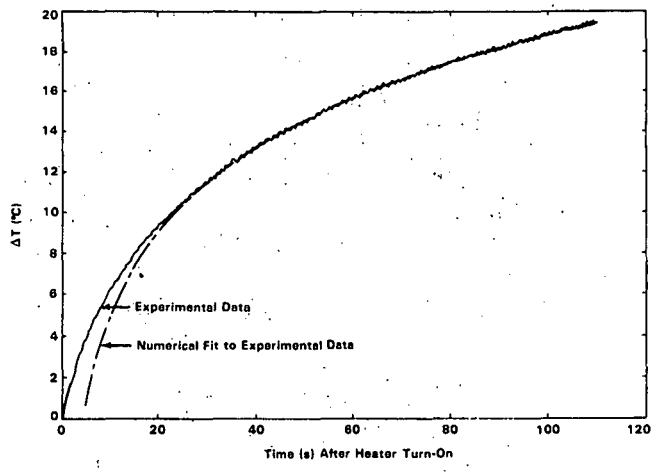

Figure B-3 ΔT-Time Plot for Data Shown in Figure B-2

Several sources of error are possible in these measurements. In some tests, contact resistance may develop between heater and rock, generally at higher temperatures. This may be reflected by either an anomalously low apparent thermal conductivity in the early portion of the time-temperature curves, or by an extended transient period. At longer times, as the volume effectively integrated in the measurements increases, the apparent conductivity should converge on the actual conductivity. At longer times, however, the assumption of infinite volume of the test sample breaks down as the temperature at the outside of the sample rises. This condition, like end effects, results in too high an apparent conductivity. Tests affected by very-near-field contact resistance are identified by an "s-shaped" or sygmoidal time-ln t response (Figure B-4), in contrast to standard or nominal curves (Figure B-2). Test showing this type of curvature, ~15% of the total number of runs, are disregarded here.

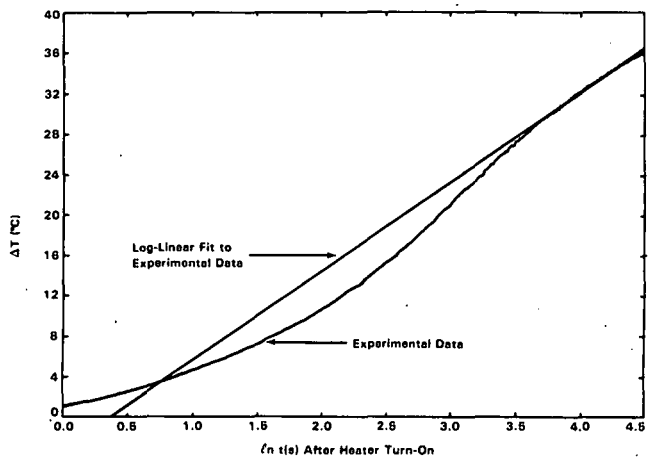

Figure B-4 ΔT-ln Time Plot, Abnormal Conductivity Test

Most of the atypical runs occurred in high-temperature measurements on either zeolitized nonwelded tuffs, or on devitrified welded tuffs from above the water table. In both cases, the source of the problem appears to be related to mineralogy.[18] Zeolitized nonwelded tuffs contract when dehydrated, while devitrifed welded tuffs above the water table frequently contain cristobalite, which goes through a large volume increase in the vicinity of 150° to 200°C. Either behavior could result in size changes in the central heater hole, and development of very-near-field contact resistance. In other cases, contact resistance might be related to fluid movement during sample dehydration. More detailed discussion of contact-resistance effects and other potential errors in transient-line-source measurements are beyond the scope of this report.

The accuracy of conductivity data generated by the transient-line-source technique depends upon the accuracy of the power factor, P, used in calculations.

This factor can be determined by two methods. First, the power supplied to the heater probe during the test can be determined by monitoring applied voltage and current, and the power factor calculated from known power input and heater length. The second approach involves testing a material of known thermal conductivity and calculating the power factor from known conductivity and measured temperature history of the heater probe.

Although no material has been adopted by the National Bureau of Standards as a standard for thermal conductivity in the range 0.5 to 4 W/m°C, fused silica has been used by many as an unofficial standard (see, for example, Ref 18). Terra Tek uses a GE No. 124 fused silica as standard. Samples of silica were prepared and tested exactly like samples of tuff, using the sample pressures, temperatures, and stabilization times. Sample geometries are identical, and the heater probe, potting material, endcaps, and jacket materials are the same for the fused silica as for the tuff samples.

Power factors in this study were routinely checked by measurements on fused silica before and after each test series, assuming an ambient-temperature conductivity of 1.33 W/m°C for the silica. Power factors were also calculated during calibrations at room temperature and pressure by monitoring power input. Factors determined by power monitoring and by measurements on fused silica agree to within ±1%. This indicates that heater performance was stable, and that, unless there is systematic error in the power monitoring, the conductivity of the fused silica is near 1.33 W/m°C.

A total of 73 measurements on fused silica were made for this study. Each assumes a constant monitored heater power factor of 130.4 to 137.0 W/m, depending upon heater. Table B-1 summarizes the results. The measured "room-temperature" thermal conductivity of the fused-silica standard, based on 25 tests and assuming predetermined power factors, is 1.326 ± 0.025 W/m°C.

Touloukian, et al[19] have compiled literature values for thermal conductivity of fused silica. As shown in Figure B-5, their "recommended" conductivity of fused silica, which they believe to be accurate to within ±3% over the temperature range shown, increases from 1.33 W/m°C at 0°C to 1.45 W/m°C at 77°C, 1.57 W/m°C at 177°C, and 1.62 W/m°C at 227°C. Both the fused-silica conductivities measured in this study and their trend with increasing temperature closely parallel data reported by Touloukian et al except near 165°C. At all other temperatures, the values reported here are the same as reported by Touloukian to within the estimated precision. This is strong confirmation of both the technique and heater power factors used here.

Table B-1 Measured Thermal Conductivity of GE No. 124 Fused Silica

Initial Temperature, T(°C)					
	23	100	165	212	260
Thermal Conductivity, K(W/m°C)					
	1.33	1.47	1.60	1.65	1.59
	1.31	1.47	1.61	1.68	1.60
	1.35	1.38	1.58	1.61	1.59
	1.34	1.39	1.58	1.63	1.59
	1.33	1.43	1.57	1.53	1.59
	1.31	1.44	1.56	1.53	1.60
	1.29	1.41	1.57	1.54	1.57
	1.30	1.44	1.62	1.58	1.64
	1.30	1.44	1.60	1.55	1.61
	1.33		1.60	1.44	1.59
	1.29		1.59	1.46	
	1.34		1.62	1.54	
	1.29			1.58	
	1.35			1.52	
	1.35			1.57	
	1.35			1.56	
	1.37			1.56	
	1.36				
	1.33				
	1.31				
	1.36				
	1.28				
	1.32				
	1.33				
	1.33				
Measurements	25	9	12	17	10
Average K	1.33	1.43	1.59	1.56	1.60
1 Std. Dev.	0.03	0.03	0.02	0.06	0.02

Three additional conductivity measurements on the standard material used in this study were made in an attempt to provide experimental confirmation of the standard's conductivity. Materials tested were cut from the same piece of silica. One sample was analyzed by Dyna Tech, Inc, in a divided-bar apparatus. Results are shown as Curve 3 in Figure B-5. The conductivities reported by Dyna Tech at low temperatures

fall very slightly below both those reported here and by Touloukian (1.29 vs 1.33 and 1.37 W/m°C at 25°C; 1.41 vs 1.43 and 1.48 W/m°C at 100°C). At higher temperatures, the conductivity reported by Dyna Tech exceeds both the values of Touloukain and those measured here. Measurements at Sandia, also by the divided-bar technique, indicate a conductivity of the GE fused silica of 1.23 W/m°C at 30°C, increasing to 1.57 W/m°C at 250°C. An additional measurement, made by J. Sass, USGS, Menlo Park, California, by the transient-line-source method is also included in Figure B-5. He reports a conductivity of 1.33 W/m°C at 25°C.

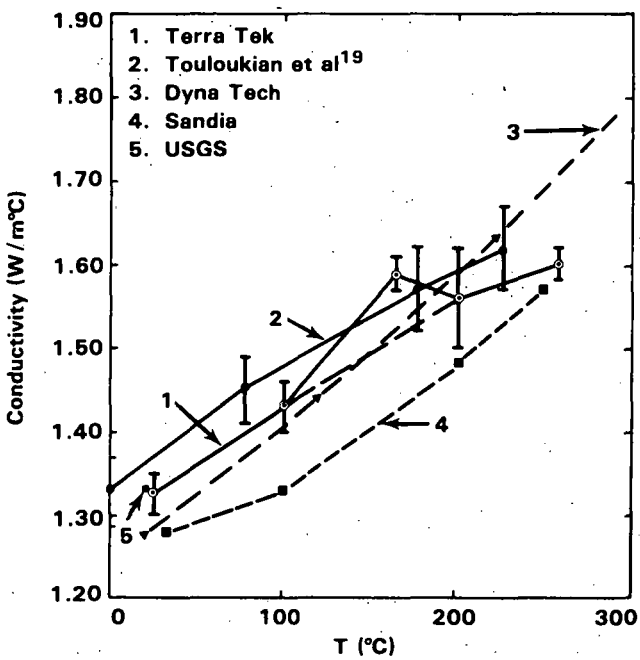

Figure B-5 Thermal Conductivity of Fused Silica

Several conclusions appear justified by these results. First, the ambient-temperature thermal conductivity of the fused-silica standard used is apparently quite near the assumed value of 1.33 W/m°C. 1.31 ± 0.06 W/m°C is the average of the four measured values and the value recommended by Touloukian. At all temperatures, the total spread between values is only about 10% of the average. Second, the trends of conductivity vs temperature measured here and reported by Touloukian are consistent. Divided-bar results at both Dyna Tech and Sandia indicate a more rapid increase in conductivity with increasing temperature. Finally, the use of ceramic cement and powdered copper as a potting compound in these measurements does apparently minimize contact resistance between heater and sample at most temperatures.

Measurements at 165°C in this study, however, are distinctly inconsistent with those at both higher and lower temperatures. The average rise in temperature during the tests was 13° to 30°C, and the boiling point of water at the fluid pressures used was near 200°C. Thus, at least a portion of the cement-copper potting mixture was raised to temperature of 180°C or greater during tests at "165°C." The cement-copper potting mix contains water. One possible reason for the apparently higher thermal conductivity near 165°C is that part of the water in the potting mixture volatilized at these temperatures, consuming energy.

In this study, it is assumed that the thermal conductivity of the fused silica increases smoothly with increasing temperature, as shown by the results of Touloukian, that the discrepancy in measurements at 165°C is due to processes in the heater/potting material only, and that the real conductivity of the Terra Tek standard at 165°C is 1.51 W/m°C instead of the measured value of 1.59 W/m°C. This is a difference of 0.08 W/m°C. Tuff conductivities at 165°C are, therefore, decreased below the measured value by 0.08 W/m°C in all data tables and figures.

APPENDIX C

Individual Thermal-Conductivity Test Results

Individual test results, both of runs accepted here and of discarded runs (see Appendix B), are included in this appendix. In all cases, the conductivity listed is that computer-calculated as the best fit for the time-delta temperature plot between 30 and 90 seconds after heater turn on. Raw data and computer plots of each individual test have been provided to Sandia National Laboratories Quality Assurance by Terra Tek, Inc, Salt Lake City.

Table C-1 Thermal-Conductivity Test Results, Topopah Springs Member, Paintbrush Tuff

Temperature (°C)	Thermal Conductivity (W/m°C) Individual Measurements	Average
Sample 795 Grain Density = 2.52 g/cm³; Porosity = 0.11		
23 (P_c = P_f = 0.1 MPa)	2.12, 2.16	2.14
(P_c = 10 MPa, P_f = 1.5 MPa)	2.14, 2.15	2.15
100 (All other tests at P_c = 10 MPa, P_f = 1.5 MPa)	2.13, 2.16	2.15
165	2.05, 2.04*	2.05*
205	1.38,** 1.30**	
270	1.21,** 1.44*	
Sample 1330 Grain Density = 2.38 g/cm³; Porosity = 0.03		
23 (All tests at P_c = 10 MPa, P_f = 1.5 MPa)	1.17, 1.18	1.18
100	1.24, 1.24	1.24
165	1.27, 1.28*	1.28*
205	1.28, 1.28	1.28
280	1.33	1.33

*Decreased by 0.08 W/m°C from raw data as discussed in Appendix B.
**This test shows double curvature in T-t plots. Data disregarded, see Appendix B.

Table C-2 Thermal-Conductivity Test Results, Tuffaceous Beds of Calico Hills

Temperature (°C)	Thermal Conductivity (W/m°C) Individual Measurements	Average
Sample 1503 Grain Density = 2.48 g/cm³; Porosity = 0.38		
23 ($P_c = P_f = 0.1$ MPa)	1.29, 1.30	1.30
($P_c = 10$ MPa, $P_f = 1.5$ MPa)	1.30, 1.30	1.30
100 (All other measurements at $P_c = 10$ MPa, $P_f = 1.5$ MPa)	1.32, 1.35	1.34
165	1.22, 1.34*	1.28*
205	0.97, 1.17**	0.97
250	0.97,** 1.02	1.02
Sample 1706 Grain Density = 2.33 g/cm³; Porosity = 0.33		
23 ($P_c = P_f = 0.1$ MPa)	1.16, 1.15	1.16
100 (All other measurements at $P_c = 10$ MPa, $P_f = 1.5$ MPa)	1.20, 1.21	1.21
165	1.22, 1.25*	1.24
210	0.86,** 0.83,** 0.82,** 0.65**	1.24

*Reduced by 0.08 W/m°C as discussed in Appendix B.
**This test shows double curvature in T-t plots. Data disregarded.

Table C-3 Thermal-Conductivity Test Results, Prow Pass Member, Crater Flat Tuff

Temperature (°C)	Thermal Conductivity (W/m°C) Individual Measurements	Average
Sample 2010 Grain Density = 2.40 g/cm³; Porosity = 0.28		
23 (P_c = P_f = 0.1 MPa)	0.93, 0.97*	–
(P_c = 10 MPa, P_f = 1.5 MPa)	1.27, 1.29	1.28
100 (All other measurements at P_c = 10 MPa, P_f = 1.5 MPa)	1.36, 1.40	1.38
165	1.46, 1.38**	1.42**
212	1.41,† 1.35,†† 1.21††	1.32
280	0.91, 0.93	0.92
Sample 2070 Grain Density = 2.41 g/cm³; Porosity = 0.29		
23 (P_c = P_f = 0.1 MPa)	1.32	1.32
(P_c = 10 MPa, P_f = 1.5 MPa)	1.34	1.34
100 (All other measurements at P_c = 10 MPa, P_f = 1.5 MPa)	1.43	1.43
165	1.47**	1.47**
212	1.00	1.00
245	0.91	0.91

*Increase in conductivity with pressure indicates ambient-pressure test affected by either contact resistance or smple collapse. Data disregarded.
**Reduced by 0.08 W/m°C from raw data as discussed in Appendix B.
†Somewhat suspect, long-time fit not good.
††Incomplete dehydration?

Table C-4 Thermal-Conductivity Test Results, Central Nonzeolitized Portion of Bullfrog Member, Crater Flat Tuff

Temperature (°C)	Thermal Conductivity (W/m°C) Individual Measurements	Average
Sample 2367.9A Grain Density = 2.59 g/cm³; Porosity = 0.25		
23 (All at P_c = 10 MPa, P_f = 1.5 MPa)	1.88, 1.87	1.88
100	1.84	1.84
165	1.76, 1.82*	1.79*
205	1.12, 1.16**	1.12
280	1.09, 1.20**	1.09
Sample 2367.9B		
23 (P_c = P_f = 0.1 MPa)	1.58, 1.62	1.60
(P_c = 10 MPa, P_f = 1.5 MPa)	1.64, 1.64	1.64
100 (All other measurements at P_c = 10 MPa, P_f = 1.5 MPa)	1.53, 1.57**	1.53
165	1.18,** 1.21**	–
212	0.67,** 0.62**	–
280	0.69**	–
Sample 2472.3 Grain Density = 2.62 g/cm³; Porosity = 0.32		
23 (All at P_c = 10 MPa, P_f = 1.5 MPa)	1.89, 1.87	1.88
100	1.82, 1.85	1.84
165	1.81, 1.87, 1.86*	1.85*
206	1.10, 1.18	1.14
260	1.15, 1.15	1.15
Sample 2473.1 Grain Density = 2.62 g/cm³; Porosity = 0.29		
23 (All at P_c = 10 MPa, P_f = 1.5 MPa)	1.79, 1.77, 1.79	1.79
100	1.74, 1.74	1.74
165	1.75, 1.76*	1.76*
206	1.04, 1.05	1.05
260	1.03, 1.03	1.03
Sample 2474.0 Grain Density = 2.62 g/cm³; Porosity = 0.31		
23 (All at P_c = 10 MPa, P_f = 1.5 MPa)	1.71, 1.72, 1.72, 1.73, 1.72, 1.71	
100	1.70, 1.71, 1.70, 1.70	1.70
165	1.69, 1.71, 1.68*	1.69*
212	1.05, 1.06	1.06
260	1.04, 1.04	1.04

Table C-4 (cont)

Temperature (°C)	Thermal Conductivity (W/m°C) Individual Measurements		Average
Sample 2493A Grain Density = 2.62 g/cm³; Porosity = 0.27			
23 ($P_c = P_f = 0.1$ MPa)	1.70,** 1.71,** 1.70**		–
($P_c = 10$ MPa, $P_f = 1.5$ MPa)	1.70**		–
100 (All other measurements at $P_c = 10$ MPa, $P_f = 1.5$ MPa)	1.85,	1.91	1.88
165	1.59,	1.63*	1.61*
Sample 2493B			
23 ($P_c = P_f = 0.1$ MPa)	1.86,	1.88	1.87
($P_c = 10$ MPa, $P_f = 1.5$ MPa)	1.92,	1.85	1.89
100 (All other measurements at $P_c = 10$ MPa, $P_f = 1.5$ MPa)	1.90,	1.89	1.90
165	1.85,	2.00*	1.93*
205	1.14,	1.16	1.15
280	1.15,	1.18	1.17
Sample 2536 Grain Density = 2.65 g/cm³; Porosity = 0.22			
23 ($P_c = P_f = 0.1$ MPa)	1.73,	1.77†	–
($P_c = 10$ MPa, $P_f = 1.5$ MPa)	1.90,	1.89	1.90
100 (All other measurements at $P_c = 10$ MPa, $P_f = 1.5$ MPa)	1.79,	1.91	1.85
165	1.84*		1.84*
212	1.33,	1.35**	1.33
280	1.29,	1.32	1.31

*Reduced by 0.08 W/m°C from raw data as discussed in Appendix B.
**This test shows double curvature. Data disregarded.
†Increase in conductivity indicates confined tests either not fully saturated or affected by contact resistance. Data disregarded.

Table C-5 Thermal-Conductivity Test Results, Zeolitized Portion of Bullfrog Member, Crater Flat Tuff

Temperature (°C)	Thermal Conductivity (W/m°C) Individual Measurements	Average
Sample 2274.4 Grain Density = 2.36 g/cm³; Porosity = 0.34		
23 ($P_c = P_f = 0.1$ MPa)	1.37	1.37
($P_c = 10$ MPa, $P_f = 1.5$ MPa)	1.37	1.37
100	1.41	1.41
165	1.42*	1.42*
212	1.09	1.09
Sample 2310 Grain Density = 2.44 g/cm³; Porosity = 0.37		
23 ($P_c = P_f = 0.1$ MPa)	1.39, 1.39, 1.36	1.38
($P_c = 10$ MPa, $P_f = 1.5$ MPa)	1.37 1.37,	1.37
100	1.43, 1.43	1.43
165	1.42, 1.44*	1.43*
212	1.08, 1.09	1.08
	1.07, 1.07	
260	1.04, 1.05	1.05
Sample 2311 Grain Density = 2.41 g/cm³; Porosity = 0.36		
23 ($P_c = P_f = 0.1$ MPa)	1.37	1.37
($P_c = 10$ MPa, $P_f = 1.5$ MPa)	1.39	1.39
100	1.43, 1.44	1.44
165	1.43, 1.45*	1.44*
215	1.11,† 1.02,	1.01
	1.00, 1.02, 1.00	
260	0.95, 0.97	0.96
Sample 2568.1 Grain Density = 2.41 g/cm³; Porosity = 0.32		
23 ($P_c = P_f = 0.1$ MPa)	1.33, 1.34	1.34
($P_c = 10$ MPa, $P_f = 1.5$ MPa)	1.35, 1.35	1.35
100	1.40, 1.38, 1.43, 1.42	1.41
165	1.47, 1.46*	1.47*
215	1.07, 1.06	1.06
260	1.03, 1.03	1.03
Sample 2569 Grain Density = 2.44 g/cm³; Porosity = 0.32		
23 ($P_c = P_f = 0.1$ MPa)	1.38, 1.40	1.39
($P_c = 10$ MPa, $P_f = 1.5$ MPa)	1.33, 1.35	1.34
100	1.42, 1.42	1.42
165	1.45, 1.43*	1.44*
215	1.18, 1.19	1.19
260	1.15, 1.15	1.15

*Reduced by 0.08 W/m°C from raw data as discussed in Appendix B.
†Single high value apparently due to incomplete sample dehydration and disregarded in averaging.

Table C-6 Thermal-Conductivity Test Results, Tram Member, Crater Flat Tuff

Temperature (°C)	Thermal Conductivity (W/m°C) Individual Measurements	Average
Sample 2701.2 Grain Density = 2.42 g/cm³; Porosity = 0.31		
23 (P_c = P_f = 0.1 MPa)	1.38	1.38
(P_c = 10 MPa, P_f = 1.5 MPa)	1.40	1.40
100	1.44	1.44
165	1.45*	1.45*
212	1.20**	1.20**
245	1.02	1.02
Sample 2814 Grain Density = 2.63 g/cm³; Porosity = 0.24		
23 (P_c = P_f = 0.1 MPa)	2.27, 2.30	2.28
(P_c = 10 MPa, P_f = 1.5 MPa)	2.23, 2.24	2.24
100	2.21, 2.26	2.24
165	2.14, 2.10*	2.12*
205	1.60,† 1.46†	–
280	1.38, 1.41	1.40
Sample 2842 Grain Density = 2.53 g/cm³; Porosity = 0.19		
23 (P_c = P_f = 0.1 MPa)	1.77,† 1.70†	–
(P_c = 10 MPa, P_f = 1.5 MPa)	1.75, 1.78	1.77
100	1.78, 1.76	1.77
165	1.71, 1.50, 1.90,† 1.76	1.66
205	0.78,† 0.79,† 0.71,† 0.73,† 0.77,† 0.77†	–
280	0.78,† 0.16†	–
Sample 2928.3 Grain Density = 2.65 g/cm³; Porosity = 0.19		
23 (P_c = 10 MPa, P_f = 1.5 MPa)	2.06, 2.08	2.07
100	2.01, 2.03, 2.01	2.02
165	2.00, 2.02*	2.01*
212	1.54, 1.56	1.55
260	1.52, 1.53, 1.52	1.52

Table C-6 (cont)

Temperature (°C)	Thermal Conductivity (W/m°C) Individual Measurements	Average
Sample 2938.8 Grain Density = 2.64 g/cm³; Porosity = 0.18		
23 (P_c = P_f = 0.1 MPa)	2.08, 2.11	2.10
(P_c = 10 MPa, P_f = 1.5 MPa)	2.09, 2.09	2.09
100	2.05, 2.09, 2.11, 2.07, 2.06	2.08
165	2.02, 2.07, 2.08*	2.06*
212	1.69,† 1.59,† 1.58, 1.54, 1.59,† 1.69,† 1.57, 1.57	1.57
260	1.56	1.56
Sample 3050 Grain Density = 2.59 g/cm³; Porosity = 0.25		
23 (P_c = P_f = 0.1 MPa)	1.94	1.94
(P_c = 10 MPa, P_f = 1.5 MPa)	1.96	1.96
100	1.98	1.98
165	1.98*	1.98*
212	1.77**	1.77**
245	1.53	1.53

*Decreased by 0.08 W/m°C from raw data as discussed in Appendix B.
**Incomplete dehydration?
†This test shows double curvature in T-t plot. Data disregarded.

APPENDIX D

Bulk-Property Measurements

This appendix contains all bulk-property measurements to date from the upper portion of Hole USW-G1. Analyses are listed in tabular form, and were determined by procedures described in Appendix A. Tables are arranged in downward stratigraphic order. Sample depths are listed only in feet, since this is the manner in which all direct drilling and coring records are kept.

Table D-1 Bulk-Property Measurements, Topopah Springs Member of Paintbrush Tuff

1. Initial density (g/cm^3)
2. Dry bulk density (g/cm^3)
3. Grain density (g/cm^3)
4. Relative weight fraction of water (on basis of initial density)
5. Porosity (calculated)
6. Saturation (calculated)
7. Bulk density at full saturation (calculated, g/cm^3)

Sample Depth (ft)	1	2	3	4	5	6	7	Lithologic Type (Generalized from Ref 1)
263.5	2.06	1.81	2.47	0.12	0.27	0.93	2.07	Nonwelded, vitric
751.8	2.23	2.06	2.51	0.08	0.18	0.94	2.24	Densely welded;
795.0	2.26	2.25	2.52	0.00	0.11	0.09	2.35	devitrified with or
810.0A	2.36	2.27	2.51	0.04	0.10	0.90	2.36	without lithophysae
810.0B	2.35	2.25	2.51	0.04	0.10	1.00	2.36	
890.3	2.36	2.25	2.54	0.05	0.11	1.00	2.36	
939.0A	2.34	2.18	2.59	0.07	0.16	1.00	2.34	
939.0B	2.30	2.20	2.51	0.04	0.12	0.83	2.33	
959.4	2.33	2.22	2.52	0.05	0.12	0.92	2.34	
1017.6	2.34	2.20	2.54	0.06	0.13	1.08	2.34	
1047.1	2.36	2.26	2.55	0.04	0.11	0.91	2.38	
1100.1	2.31	2.17	2.54	0.06	0.15	0.93	2.31	
1151.1	2.30	2.16	2.56	0.06	0.16	0.88	2.31	
1210.7	2.34	2.25	2.54	0.04	0.11	0.82	2.37	
1245.0	2.40	2.33	2.58	0.03	0.10	0.70	2.42	
1288.4	2.35	2.32	2.41	0.01	0.04	0.75	2.35	Densely welded vitric,
1330.0A	2.32	2.31	2.38	0.01	0.03	0.33	2.34	the "basal vitrophyre"
1330.0B	2.31	2.30	2.38	0.01	0.03	0.33	2.34	
1330.0C	2.32	2.30	2.39	0.01	0.04	0.50	2.33	
1332.8	2.34	2.31	2.40	0.01	0.04	0.75	2.34	
1385.2	1.91	1.59	2.37	0.17	0.33	0.97	1.92	Partially welded to non-welded

Table D-2 Bulk-Property Measurements, Tuffaceous Beds of Calico Hills

1. Initial density (g/cm³)
2. Dry bulk density (g/cm³)
3. Grain density (g/cm³)
4. Relative weight fraction of water (on basis of initial density)
5. Porosity (calculated)
6. Saturation (calculated)
7. Bulk density at full saturation (calculated, g/cm³)

Sample Depth (ft)	1	2	3	4	5	6	7	Lithologic Type (Generalized from Ref 1)
1469.9	1.89	1.53	2.41	0.19	0.37	0.97	1.89	Nonwelded ashflow
1503.0	1.85	1.53	2.48	0.21	0.38	0.84	1.92	
1505.0	1.86	1.57	2.28	0.16	0.31	0.94	1.88	
1514.8	1.93	1.60	2.40	0.17	0.33	1.00	1.94	
1553.0	1.76	1.49	2.30	0.16	0.35	0.77	1.85	Nonwelded ashflow
1571.2	1.85	1.47	2.40	0.21	0.39	0.97	1.85	Nonwelded ashflow
1606.0A	1.86	1.51	2.47	0.19	0.39	0.90	1.90	
1606.0B	1.71	1.55	2.24	0.10	0.31	0.52	1.86	
1606.0C	1.71	1.56	2.24	0.09	0.30	0.50	1.87	
1606.0D	1.77	1.53	2.25	0.13	0.32	0.75	1.85	
1652.0A	1.70	1.53	2.38	0.08	0.36	0.47	1.88	
1652.0B	1.88	1.57	2.33	0.20	0.33	0.94	1.89	
1663.5	1.95	1.63	2.45	0.17	0.33	0.97	1.97	
1667.0	1.92	1.58	2.44	0.18	0.35	0.97	1.94	
1705.5	1.88	1.57	2.33	0.16	0.33	0.94	1.89	Nonwelded ashflow
1722.3	1.93	1.58	2.48	0.18	0.36	0.97	1.95	
1784.5	2.24	2.00	2.62	0.11	0.24	1.00	2.24	Bedded/reworked, including tuffaceous sandstone

Table D-3 Bulk-Property Measurements, Prow Pass Member, Crater Flat Tuff

1. Initial density (g/cm³)
2. Dry bulk density (g/cm³)
3. Grain density (g/cm³)
4. Relative weight fraction of water (on basis of initial density)
5. Porosity (calculated)
6. Saturation (calculated)
7. Bulk density at full saturation (calculated, g/cm³)

Sample Depth (ft)	1	2	3	4	5	6	7	Lithologic Type (Generalized from Ref 1)
1832.0A	1.88	1.55	2.38	0.17	0.35	0.94	1.90	Partially welded
1832.0B	1.88	1.52	2.37	0.19	0.36	1.00	1.88	ashflow; devitrified
1847.0A	1.91	1.56	2.42	0.18	0.36	0.97	1.91	
1847.0B	1.91	1.56	2.46	0.19	0.37	0.95	1.92	
1886.0	2.09	1.77	2.59	0.15	0.32	1.00	2.08	Partially to moderately
1926.6	1.97	1.78	2.63	0.10	0.32	0.59	2.11	welded ashflow;
1930.0	2.01	1.67	2.55	0.17	0.35	0.97	2.01	devitrified
1947.0	2.07	1.96	2.51	0.08	0.22	0.50	2.18	
1948.0	1.91	1.90	2.56	0.01	0.26	0.04	2.15	
1973.7	2.05	1.75	2.52	0.15	0.31	0.97	2.05	
2010.0A	2.03	1.78	2.37	0.14	0.25	1.00	2.03	Partially welded
2010.0B	1.93	1.66	2.42	0.14	0.31	0.87	1.98	ashflow; devitrified
2050.0	1.98	1.71	2.38	0.14	0.28	0.96	1.99	
2052.0	1.98	1.67	2.46	0.16	0.32	0.97	1.99	
2064.9	1.89	1.73	2.37	0.09	0.27	0.59	2.00	
2065.0	1.93	1.67	2.36	0.13	0.29	0.90	1.97	
2066.0	1.98	1.69	2.39	0.15	0.29	1.00	1.98	
2067.0	2.03	1.75	2.43	0.14	0.28	1.00	2.03	
2070.0	1.96	1.72	2.41	0.12	0.29	0.83	2.00	
2086.0	1.89	1.64	2.40	0.14	0.32	0.78	1.95	Partially to moderately
2113.0	1.99	1.69	2.38	0.15	0.29	1.03	1.98	welded ashflow;
2128.0	1.92	1.65	2.41	0.14	0.32	0.84	1.96	devitrified
2151.0	2.00	1.74	2.35	0.13	0.26	1.00	2.00	
2170.0A	2.05	1.78	2.46	0.13	0.28	0.96	2.05	Bedded/reworked, with
2170.0B	2.07	1.82	2.47	0.12	0.27	0.96	2.07	tuffaceous sandstone

Table D-4 Bulk-Property Measurements, Bullfrog Member, Crater Flat Tuff

1. Initial density (g/cm³)
2. Dry bulk density (g/cm³)
3. Grain density (g/cm³)
4. Relative weight fraction of water (on basis of initial density)
5. Porosity (calculated)
6. Saturation (calculated)
7. Bulk density at full saturation (calculated, g/cm³)

Sample Depth (ft)	1	2	3	4	5	6	7	Lithologic Type (Generalized from Ref 1)
2192.0	1.99	1.70	2.46	0.15	0.31	0.94	2.01	Nonwelded ashflow; devitrified
2206.0	1.91	1.64	2.43	0.14	0.33	0.82	1.96	
2227.0	1.86	1.50	2.44	0.20	0.39	0.92	1.88	Nonwelded to partially welded ashflow
2232.0	1.82	1.50	2.44	0.20	0.39	0.97	1.88	
2261.0	1.89	1.54	2.41	0.19	0.36	0.98	1.90	
2265.0	1.88	1.55	2.44	0.18	0.36	0.92	1.92	
2273.4	1.91	1.57	2.43	0.18	0.35	0.97	1.93	
2274.4A	1.85	1.58	2.31	0.17	0.32	0.84	1.89	
2274.4B	1.89	1.56	2.40	0.18	0.35	0.94	1.91	
2276.0	1.92	1.58	2.40	0.18	0.34	1.00	1.00	
2285.0	1.87	1.52	2.40	0.19	0.37	0.95	1.88	
2286.0	1.88	1.54	2.39	0.18	0.36	0.94	1.89	
2310.2A	1.85	1.51	2.40	0.18	0.37	0.92	1.88	
2310.2B	1.87	1.51	2.47	0.19	0.39	0.92	1.90	
2310.8A	1.88	1.54	2.39	0.18	0.36	0.94	1.89	
2310.8B	1.87	1.51	2.48	0.20	0.39	0.92	1.90	
2311.5A	1.85	1.51	2.35	0.18	0.36	0.94	1.86	
2311.5B	1.90	1.57	2.47	0.17	0.36	0.92	1.94	
2312.0	1.87	1.52	2.37	0.19	0.36	0.99	1.88	
2313.0	1.85	1.49	2.42	0.20	0.39	0.92	1.87	
2321.0A	1.91	1.61	2.54	0.16	0.37	0.81	1.97	Partially welded ashflow; vapor phase zone
2321.0B	1.90	1.62	2.54	0.17	0.36	0.78	1.99	
2321.0C	1.92	1.63	2.54	0.18	0.36	0.81	1.99	
2321.0D	1.89	1.60	2.54	0.18	0.37	0.78	1.97	
2321.0E	1.93	1.63	2.56	0.18	0.37	0.81	1.98	
2321.0F	1.90	1.61	2.58	0.15	0.38	0.76	1.98	
2332.0	1.96	1.64	2.58	0.17	0.37	0.86	2.00	
2338.0A	1.95	1.60	2.65	0.18	0.40	0.88	1.99	
2338.0B	1.95	1.61	2.69	0.18	0.40	0.85	2.01	
2338.0C	1.96	1.62	2.67	0.17	0.39	0.87	2.02	
2338.0D	2.00	1.66	2.69	0.17	0.39	0.87	2.03	
2338.0E	1.98	1.64	2.66	0.17	0.38	0.89	2.03	
2338.0F	1.97	1.63	2.70	0.17	0.40	0.85	2.02	
2338.0G	1.98	1.66	2.62	0.16	0.37	0.86	2.02	
2338.0H	1.98	1.66	2.66	0.17	0.38	0.84	2.03	
2355.0	2.07	1.84	2.64	0.11	0.30	0.77	2.15	
2355.9	2.12	1.87	2.60	0.13	0.28	0.89	2.15	
2367.9	2.12	1.95	2.59	0.08	0.25	0.68	2.19	
2371.0	2.17	1.91	2.62	0.12	0.27	0.96	2.18	
2380.0	2.17	1.93	2.55	0.11	0.24	0.99	2.18	

Table D-4 (cont)

Sample Depth (ft)	1	2	3	4	5	6	7	Lithologic Type (Generalized from Ref 1)
2382.9	2.18	1.92	2.60	0.12	0.26	1.00	2.18	
2385.3A	2.17	1.93	2.66	0.11	0.27	0.89	2.21	
2385.3B	2.15	1.94	2.65	0.11	0.27	0.78	2.20	
2385.3C	2.12	1.89	2.64	0.11	0.28	0.82	2.18	
2385.3D	2.13	1.90	2.61	0.11	0.27	0.85	2.18	
2385.3E	2.12	1.88	2.64	0.11	0.29	0.83	2.16	
2392.0	2.21	1.95	2.62	0.12	0.26	1.00	2.21	
2405.0	2.18	1.92	2.61	0.12	0.26	1.00	2.18	
2405.8	2.18	1.93	2.59	0.12	0.25	1.00	2.18	
2414.0A	2.14	1.86	2.61	0.13	0.29	0.97	2.14	
2414.0B	2.14	1.88	2.57	0.12	0.27	0.96	2.15	
2428.0A	2.08	1.83	2.62	0.14	0.30	0.83	2.13	
2428.0B	2.10	1.86	2.62	0.13	0.29	0.83	2.15	
2428.0C	2.13	1.87	2.65	0.14	0.29	0.90	2.17	
2428.0D	2.14	1.89	2.62	0.13	0.28	0.89	2.17	
2428.0E	2.13	1.82	2.64	0.13	0.31	1.00	2.13	
2428.0F	2.14	1.89	2.64	0.14	0.28	0.89	2.18	
2428.0G	2.10	1.87	2.62	0.12	0.29	0.79	2.15	
2428.0H	2.10	1.87	2.61	0.12	0.28	0.82	2.16	
2428.0I	2.08	1.83	2.62	0.14	0.30	0.83	2.13	
2428.0J	1.95	1.72	2.63	0.13	0.35	0.66	2.06	
2428.0K	2.14	1.89	2.63	0.13	0.28	0.89	2.17	
2429.0A	2.17	1.90	2.62	0.13	0.28	0.99	2.17	
2429.0B	2.16	1.89	2.60	0.13	0.27	1.00	2.16	
2445.0	2.20	1.95	2.63	0.11	0.26	0.96	2.21	
2468.0	2.15	1.94	2.60	0.13	0.28	0.99	2.15	Moderately to densely welded ashflow; devitrified
2472.3A	2.06	1.81	2.60	0.14	0.30	0.83	2.12	
2472.3B	2.02	1.74	2.64	0.12	0.34	0.82	2.08	
2472.5A	2.14	1.89	2.63	0.12	0.28	0.89	2.17	
2472.5B	2.18	1.93	2.65	0.11	0.27	0.93	2.20	
2473.5A	2.11	1.87	2.61	0.11	0.28	0.86	2.16	
2473.5B	2.13	1.88	2.63	0.12	0.29	0.86	2.16	
2474.0A	2.06	1.81	2.62	0.12	0.31	0.81	2.12	
2474.0B	2.08	1.83	2.62	0.12	0.30	0.83	2.13	
2480.0	2.18	1.94	2.61	0.11	0.26	0.92	2.19	
2485.6	2.20	1.97	2.57	0.11	0.23	1.00	2.20	
2493.0A	2.15	1.91	2.62	0.13	0.27	0.89	2.18	
2493.0B	2.17	1.94	2.61	0.12	0.26	0.88	2.19	
2501.0	2.21	1.99	2.61	0.10	0.24	0.92	2.22	
2509.0	2.22	2.02	2.62	0.09	0.23	0.87	2.25	
2510.0	2.17	1.95	2.54	0.10	0.23	0.94	2.19	
2517.0	2.29	2.10	2.62	0.08	0.20	0.95	2.30	
2518.0	2.27	2.07	2.60	0.09	0.20	1.00	2.27	
2530.0	2.28	2.09	2.61	0.08	0.20	0.95	2.29	
2536.2A	2.19	2.03	2.66	0.08	0.24	0.67	2.26	
2536.2B	2.27	2.11	2.63	0.10	0.20	0.80	2.30	Moderately to partially welded ashflow; devitrified
2538.0	2.20	1.97	2.58	0.11	0.24	0.99	2.20	
2549.0	1.92	1.69	2.48	0.12	0.32	0.72	2.01	

Table D-4 (cont)

Sample Depth (ft)	1	2	3	4	5	6	7	Lithologic Type (Generalized from Ref 1)
2550.0	2.05	1.80	2.43	0.12	0.26	0.97	2.06	
2551.5	2.07	1.87	2.46	0.10	0.24	0.83	2.11	
2561.0	2.09	1.86	2.43	0.11	0.23	1.00	2.09	
2563.0	2.15	1.94	2.47	0.10	0.21	0.98	2.16	
2568.1A	1.96	1.69	2.36	0.14	0.28	0.96	1.98	
2568.1B	1.96	1.68	2.46	0.14	0.32	0.88	1.99	
2568.7A	1.95	1.70	2.38	0.13	0.29	0.86	1.98	
2568.7B	1.97	1.68	2.53	0.15	0.34	0.85	2.01	
2569.1A	1.92	1.67	2.38	0.13	0.30	0.83	1.97	
2569.1B	1.95	1.66	2.49	0.15	0.33	0.88	2.00	
2585.0	2.04	1.81	2.39	0.11	0.24	0.95	2.06	
2587.0	2.04	1.79	2.44	0.13	0.27	0.93	2.05	
2588.0	2.05	1.79	2.44	0.13	0.27	0.96	2.05	
2607.0	2.06	1.82	2.44	0.12	0.25	0.96	2.08	Bedded/reworked tuff
2608.0	2.12	1.89	2.47	0.11	0.24	0.98	2.12	

Table D-5 Bulk-Property Measurements, Tram Member, Crater Flat Tuff

1. Initial density (g/cm^3)
2. Dry bulk density (g/cm^3)
3. Grain density (g/cm^3)
4. Relative weight fraction of water (on basis of initial density)
5. Porosity (calculated)
6. Saturation (calculated)
7. Bulk density at full saturation (calculated, g/cm^3)

Sample Depth (ft)	1	2	3	4	5	6	7	Lithologic Type (Generalized from Ref 1)
2641.0	2.07	1.80	2.49	0.13	0.28	0.99	2.07	
2653.0	2.00	1.71	2.44	0.15	0.30	0.97	2.01	Partially to moderately
2658.4	1.97	1.69	2.44	0.17	0.31	0.90	1.99	welded ashflow;
2658.6	2.02	1.79	2.31	0.12	0.23	1.00	2.02	devitrified
2658.8	1.96	1.70	2.32	0.14	0.27	0.96	1.96	
2659.0	2.08	1.86	2.37	0.17	0.22	1.00	2.08	
2659.4	1.92	1.70	2.39	0.12	0.29	0.76	1.99	
2691.0	2.09	1.87	2.43	0.11	0.23	0.96	2.10	
2701.2A	1.96	1.70	2.42	0.15	0.30	0.87	1.99	
2701.2B	1.96	1.67	2.41	0.15	0.31	0.94	1.97	
2725.0	2.03	1.74	2.44	0.14	0.29	1.00	2.03	
2761.0	2.15	1.89	2.61	0.12	0.28	0.93	2.16	
2794.0	2.29	2.11	2.63	0.08	0.20	0.90	2.30	
2814.0A	2.21	2.00	2.63	0.10	0.24	0.88	2.24	
2814.0B	2.16	1.96	2.64	0.10	0.26	0.77	2.21	
2814.0C	2.23	2.07	2.64	0.08	0.22	0.73	2.28	
2814.0D	2.21	2.03	2.61	0.09	0.22	0.82	2.26	
2830.0	2.25	2.04	2.64	0.10	0.23	0.91	2.26	

Table D-5 (cont)

Sample Depth (ft)	1	2	3	4	5	6	7	Lithologic Type (Generalized from Ref 1)
2842.0	2.25	2.06	2.53	0.09	0.19	1.00	2.25	
2847.8	2.35	2.18	2.62	0.07	0.17	1.00	2.35	
2861.0	2.23	1.99	2.64	0.11	0.25	0.96	2.23	
2897.0	2.26	2.05	2.64	0.09	0.22	0.95	2.28	
2928.1A	2.31	2.17	2.65	0.06	0.18	0.78	2.35	
2928.1B	2.32	2.14	2.65	0.08	0.19	0.95	2.34	
2938.8	2.31	2.14	2.63	0.07	0.19	0.89	2.32	
2939.3	2.34	2.18	2.64	0.07	0.17	0.94	2.36	
2943.0	2.37	2.21	2.63	0.06	0.16	1.00	2.37	
2952.0	2.41	2.29	2.64	0.05	0.13	0.92	2.43	
2970.0	2.32	2.15	2.64	0.08	0.19	0.89	2.33	
3006.0	2.28	2.08	2.61	0.09	0.20	1.00	2.28	
3041.0	2.13	1.89	2.52	0.11	0.25	0.96	2.14	
3050.0A	2.13	1.97	2.61	0.08	0.25	0.64	2.21	
3050.0B	2.11	1.89	2.57	0.11	0.27	0.89	2.15	
3051.0A	2.38	2.24	2.61	0.06	0.14	1.00	2.38	
3051.0B	2.31	2.11	2.62	0.08	0.19	1.05	2.31	
3084.0	2.20	1.97	2.61	0.11	0.25	0.92	2.21	Partially welded ash-flow; zeolitized
3085.0	2.30	2.10	2.63	0.09	0.20	1.00	2.30	
3102.0	2.13	1.87	2.50	0.11	0.25	0.92	2.13	
3106.8	2.11	1.88	2.50	0.11	0.25	0.92	2.13	
3107.4	2.11	1.88	2.48	0.11	0.24	0.96	2.12	
3150.0	2.24	2.05	2.58	0.09	0.21	0.90	2.25	Nonwelded to partially welded ashflow; zeolitized and argillic
3173.6	2.33	2.15	2.65	0.08	0.19	0.95	2.34	
3200.0A	2.32	2.15	2.61	0.07	0.18	0.94	2.32	
3200.0B	2.33	2.17	2.63	0.07	0.17	0.94	2.35	
3226.6	2.31	2.11	2.64	0.09	0.20	1.00	2.31	
3251.0	2.29	2.08	2.63	0.09	0.21	1.00	2.29	
3297.0	2.32	2.13	2.62	0.08	0.19	1.00	2.32	
3325.8	2.31	2.09	2.68	0.09	0.22	1.00	2.31	
3350.0	2.34	2.16	2.62	0.08	0.18	1.00	2.34	
3400.0	2.37	2.20	2.68	0.07	0.18	0.94	2.38	
3426.8	2.35	2.18	2.70	0.07	0.19	0.89	2.38	
3448.0	2.36	2.17	2.71	0.08	0.20	0.95	2.37	
3495.9	2.39	2.20	2.75	0.08	0.20	0.95	2.40	
3498.0	2.38	2.18	2.72	0.08	0.20	1.00	2.38	

References

[1]R. W. Spengler, F. M. Byers, Jr, and J. B. Waren, *Stratigraphy and Structure of Volcanic Rocks in Drill Hole USW-G1, Yucca Mountain, Nye County, Nevada*, US Geological Survey, Open-File Report 81-1349, in preparation.

[2]R. W. Spengler, D. C. Muller, and R. B. Livermore, *Preliminary Report on the Geology and Geophysics of Drill Hole UE25A#1, Yucca Mountain, Nevada Test Site*, US Geological Survey Open-File Report 79-1244 (Denver, CO: US Geological Survey, 1979).

[3]W. Woodside and J. H. Messmer, "Thermal Conductivity of Porous Media," I. Unconsolidated Sands, *J App Phys* 32:1688-98, 1961.

[4]P. W. Lipman, R. L. Christiansen, and J. T. O'Conner, *A Compositionally Zoned Ash-Flow Sheet in Southern Nevada*, US Geological Survey, Prof. Pap. 524-F (Washington, DC: US Government Printing Office, 1966).

[5]M. L. Sykes, G. H. Heiken, and J. R. Smyth, *Mineralogy and Petrology of Tuff Units From the UE25a-1 Drill Site, Yucca Mountain, Nevada*, Informal Report LA-8139-MS (Los Alamos, NM: Los Alamos National Laboratory, 1979).

[6]P. R. Carroll, and A. C. Waters, editors, *Preliminary Stratigraphic and Petrologic Characterization of Core Samples From USW-G1, Yucca Mountain, Nevada*, Informal Report LA-8840-MS (Los Alamos, NM: Los Alamos National Laboratory, 1981).

[7]N. B. C. Yelamanchili, memo to A. R. Lappin, SNLA dtd. 10/23/80: "Thermal Conductivity of Tuff Samples," Holmes and Narver, Inc, Materials Testing Laboratory, Nevada Test Site.

[8]N. B. C. Yelamanchili, memo to A. R. Lappin, SNLA dtd. 3/12/80: "Thermal Conductivity and Physical Properties Test Results on Tuff Specimens from Drill Hole UE25A#1," Holmes and Narver, Inc, Materials Testing Laboratory, Nevada Test Site, Laboratory Report No. 584.

[9]A. R. Lappin, *Thermal Conductivity of Silicic Tuffs: Predictive Formalism and Comparison With Preliminary Experimental Results*, SAND80-0769 (Albuquerque, NM: Sandia National Laboratories, 1980).

[10]N. B. C. Yelamanchili, memo to A. R. Lappin, SNLA dtd. 7/31/79: "Thermal Conductivity Test on Tuff Samples From UE25A#1 Drill Hole," Holmes and Narver, Inc, Materials Testing Laboratory, Nevada Test Site, Laboratory Report No. 2068.

[11]F. M. Byers, Jr, et al, *Volcanic Suites and Related Cauldrons of Timber Mountain - Oasis Valley Caldera Complex, Southern Nevada*, US Geological Survey, Prof. Pap. 919 (Washington, DC: US Government Printing Office, 1976).

[12]J. H. Sass, A. H. Lachenbrush, and R. J. Munroe, "Thermal Conductivity of Rocks From Measurements on Fragments and its Applications to Heat-Flow Determinations;" *J Geoph Res* 76:3391-3401, 1971.

[13]E. C. Robertson and D. L. Peck, "Thermal Conductivity of Vesicular Basalt From Hawaii;" *J Geoph Res* 79:4875-88, 1974.

[14]W. Woodside and J. H. Messmer, "Thermal Conductivity of Porous Media II. Consolidated Rocks;" *J App Phys* 32:1699-1706, 1961.

[15]J. Kestin, "Thermal Conductivity of Water and Steam;" *Mech Eng* 100:46-48, 1978.

[16]E. R. G. Eckert and R. M. Drake, Jr, *Analysis of Heat and Mass Transfer* (New York: McGraw-Hill, 1972).

[17]A. R. Lappin, *Preliminary Thermal Expansion Screening Data for Tuffs*, SAND78-1147 (Albuquerque, NM: Sandia National Laboratories, 1980).

[18]W. L. Sibbitt, J. G. Dodson, and J. W. Tester, "Thermal Conductivity of Crystalline Rocks Associated With Energy Extraction From Hot Dry Rock Geothermal Systems," *J Geoph Res* 84:B.3, p 1117-24, 1979.

[19]Y. S. Touloukian, et al, "Thermal Conductivity, Nonmetallic Solids; Thermophysical Properties of Matter," V 2 IFI/Plenum, New York, 1970.

DISTRIBUTION:

TIC-4500 (R69) UC-70 (325)

US Department of Energy (3)
Office of Waste Isolation
Germantown, MD 20767
Attn: W. Ballard, Director
Rm B-207
C. R. Cooley, Deputy Director
Rm B-214
R. Stein, Actg Team Leader
Tech Team, Rm B-220

US Department of Energy
National Waste Terminal Storage Program Office
505 King Ave.
Columbus, OH 43201
Attn: J. O. Neff, Program Manager

Lawrence Livermore National Lab (3)
PO Box 808
Livermore, CA 94550
Attn: L. D. Ramspott
Technical Project Officer, MS L-204
K. Street, Jr, MS L-209
A. J. Rotham, MS L-204

Los Alamos National Lab (2)
PO Box 1663
Los Alamos, NM 87545
Attn: B. R. Erdal
Technical Project Officer, MS 514
D. C. Hoffman, MS 760

Westinghouse – AESD
PO Box 708
Mercury, NV 89023
Attn: A. R. Hakl
Site Manager, MS 703

US Geological Survey (2)
PO Box 25046
Federal Center
Denver, CO 80301
Attn: G. L. Dixon
Technical Project Officer, MS 954
W. E. Wilson, MS 954

W. S. Twenhofel
820 Estes St
Lakewood, CO 80226

US Department of Energy
Richland Operations Office
PO Box 550
Richland, WA 99352
Attn: R. G. Goranson

Rockwell International Atomics International Division
Rockwell Hanford Operations
Richland, WA 99352
Attn: R. Deju

US Department of Energy (13)
PO Box 14100
Las Vegas, NV 89114
Attn: R. M. Nelson, Director (3)
Waste Mgmt Project Office
D. F. Miller, Director
Office of Public Affairs
R. H. Marks, CP-1, MS 210
B. W. Church, Director
Health Physics Division
R. R. Loux (7)

Holmes & Narver, Inc
PO Box 14340
Las Vegas, NV 89114
Attn: A. E. Gurrola

Batelle (8)
505 King Ave
Columbus, OH 43201
Attn: Office of Nuclear Waste Isolation, For
N. E. Carter
S. Goldsmith
ONWI Library (5)
Office of NWTS Integration For
W. A. Carbiener

State of Nevada
Capitol Complex
Governor's Office of Planning Coordination
Carson City, NV 89023
Attn: R. M. Hill
State Planning Coordinator

DISTRIBUTION (cont):

Department of Energy
State of Nevada
Capitol Complex
Carson City, NV 89710
Attn: N. A. Clark

International Atomic Energy Agency
Div of Nuclear Power & Reactors
Karnter Ring 11
PO Box 590, A-1011
Vienna, AUSTRIA
Attn: J. P. Colton

Reynolds Electrical & Engineering Co., Inc
MS 555
PO Box 14400
Las Vegas, NV 89114
Attn: H. D. Cunningham

Fenix & Scisson, Inc
PO Box 15408
Las Vegas, NV 89114
Attn: J. A. Cross

Argonne National Labs
9700 S. Cass Ave.
Argonne, IL 60439
Attn: A. M. Friedman

1417 F. W. Muller
4700 E. H. Beckner
4760 R. W. Lynch
4761 L. W. Scully
4762 L. D. Tyler
4763 J. R. Tillerson
4763 D. R. Fortney
4763 A. R. Lappin (32)
4763 R. M. Zimmerman
4764 R. C. Lincoln
4764 A. E. Stephenson
5521 R. K. Thomas
5532 R. H. Price
5824 J. A. Koski
5824 M. Moss
8214 M. A. Pound
3141 L. J. Erickson (5)
3151 W. L. Garner (3)

Org.	Bldg.	Name	Rec'd by	Org.	Bldg.	Name	Rec'd by

Sandia National Laboratories